Distribution Agreement

In presenting this thesis or dissertation as a partial fulfillment of the requirements for an advanced degree from Emory University, I hereby grant to Emory University and its agents the non-exclusive license to archive, make accessible, and display my thesis or dissertation in whole or in part in all forms of media, now or hereafter known, including display on the world wide web. I understand that I may select some access restrictions as part of the online submission of this thesis or dissertation. I retain all ownership rights to the copyright of the thesis or dissertation. I also retain the right to use in future works (such as articles or books) all or part of this thesis or dissertation.

Signature:

_____ _____

Mahajabin Rahman Date

Analysis of avalanches in the landscape of disordered systems

By
Mahajabin Rahman
Doctor of Philosophy
Physics

Stefan Boettcher, Ph.D.
Advisor

Eric Weeks, Ph.D.
Committee Member

Connie Roth, Ph.D.
Committee Member

Gordon Berman, Ph.D.
Committee Member

Michelangelo Grigni, Ph.D.
Committee Member

Accepted:

Kimberly Jacob Arriola, Ph.D.
Dean of the James T. Laney School of Graduate Studies

Date

Analysis of avalanches in the landscape of disordered systems

By

Mahajabin Rahman
B.A., University of Chicago, IL, 2014

Advisor: Stefan Boettcher, Ph.D.

An abstract of
A dissertation submitted to the Faculty of the
James T. Laney School of Graduate Studies of Emory University
in partial fulfillment of the requirements for the degree of
Doctor of Philosophy
in Physics
2023

Analysis of avalanches in the landscape of disordered systems
By Mahajabin Rahman

The construct of an energy landscape makes it possible to use the same physics machinery to study completely unrelated scenarios, like fitness landscapes in evolution and algorithmic complexity in constraint satisfaction problems. I use this construct to study disordered (particularly, glassy) systems. When a thermal quench is used to access the inherent structure of their landscape, the consequence is aging – a relaxation process that exhibits interesting behaviors like memory effects, that can ideally be harnessed for engineering purposes, but the slow time-scales make this process difficult and tedious to study.

My dissertation starts and ends with the archetypal models of complex systems - the mean field Ising model called the Sherrington Kirkpatrick spin glass, and a sparse lattice model called the Edwards-Anderson spin glass. The first part of my thesis employs these models to study the statistical signatures of this relaxation process, which reflects the hierarchy of time scales of the energy landscape being explored. My research is anchored on a phenomenological description known as record dynamics (RD), which argues that large fluctuations (also called quakes or avalanches) – the rare events, rather than the averaged events – can exclusively be used to describe the relaxation process. I show that an RD-borne minimal model can reproduce even anomalous effects quintessential to aging, offering a simple alternative to mean field theoretic tools.

The second part of my thesis explores how critical avalanches are produced. Inspired by the idea that saturation bounds of marginally stable spins are indicators of whether avalanches will be critical, I use different modes of hysteretic driving to study the effects of dislodging the stability distribution to different extents. This helps drive the Edwards Anderson spin model, a difficult problem to solve (specifically NP hard), into a percolation transition, and elucidates the consequent changing correlation structure. In addition, I explore attempts to further understand the relationship between marginal stability and information transmission, and leave some open ended questions.

Analysis of avalanches in the landscape of disordered systems

By

Mahajabin Rahman
B.A., University of Chicago, IL, 2014

Advisor: Stefan Boettcher, Ph.D.

A dissertation submitted to the Faculty of the
James T. Laney School of Graduate Studies of Emory University
in partial fulfillment of the requirements for the degree of
Doctor of Philosophy
in Physics
2023

Acknowledgments

Figure 1: When I first started to work with Stefan, he used the phrase "throw the baby out with the bath water" a lot, to describe the risk of mean-field assumptions.

First, I thank my adviser Professor Stefan Boettcher for giving me a chance. I am not especially patient and need interestingness to be hurled at me, so piece-meal science is uncomfortable, as questions can lead to a deep-dive into something that may ultimately turn out to be boring. Stefan showed me what it means to have grace when taking this dive, to have a positive attitude about having spent time reading papers that ultimately turn out to be irrelevant, to place a larger premium about the truth in science, rather than how to make our own hypothesis true so that scientific defeats don't feel ruinous, and how all the above can help me build a more positive attitude towards science, and myself.

I thank my committee (Professors Gordon Berman, Michelangelo Grigni, Connie Roth and Eric Weeks). I want to emphasize that their help has not been passive throughout grad school. Connie helped me put my committee together when I felt hopelessly behind with qualifiers. Even afterwards, I have had several conversations with her about the dispiriting sense of sometimes losing enthusiasm and passion in

research, and she responded with such openness and kindness. I have never done research with Eric but learned a lot about how he thinks from semi-monthly meetings with him, which he so generously offered to have with me to help lessen my isolation being in otherwise one person group. I realized that Eric is incredibly methodical, and he very wisely evaluates the trade-offs of pursuing an idea before biting the bullet (unlike me). I remind myself these days to be more like him.

Emory folks who are not in my committee have made life meaningful here as well (in particular, I always have have fun conversations with Sergei Urazhdin, whose classical mechanics course I could not pass the first time, and passed by .04 the second time – so in truth, I should not even be here. Sergei has seen me at my worst, but remained encouraging. I thank all the Emory staff – especially Barbara Conner, who tried to help me in every way possible without ever expressing the slightest annoyance. The last of the Emory bunch I want to thank are my friends and colleagues, to whom the fun aspects of graduate school are ascribed to.

It would be atrocious to not mention my best friends Vicki and Rachel, who have not lived in the same city as me since college but have put up with my highly random dyspeptic thoughts and fixations on a nearly daily basis.

Finally, and to my great disappointment, I do not actually have words to express my gratitude to the people who – in my heart and my core, I know – I am thankful for the most: my parents, and my little brother, who never had any of the opportunities I have had. My parents made major sacrifices for me and have never asked me for anything because they wanted me to prioritize my education first. I used to think that I would look out for my little brother, but it has been the other way around – my brother looks out for everyone, and I look up to him.

Thank you to anyone who has shown me the richness of compassion, and how to combine that compassion with science.

Contents

List of Figures

Chapter 1

General Introduction

"the discovery that two events, symbols, thoughts or texts, while so utterly separated by time and space that they could not "really" be connected, seem nevertheless, to be the same or to be speaking directly to one another raises the possibility of a secret interconnection of things that is the scholar's most cherished article of faith" - J.Z Smith, The Bare Facts of Ritual

1.1 The trouble with bridging disordered systems

The notion of disorder serves as a bridge between disparate subjects [1]; disorder is fodder for artists to find "beauty" in, against the backdrop of disharmony, writers to make sense of with words, and scientists to be perpetually puzzled by, and yet, it is unclear what exactly bridges disordered systems. When far from equilibrium, disordered systems are especially challenging to study as they are excluded from the assumptions made in traditional (equilibrium) physics. Primarily, the appeal of physics is that the invariant nature of certain principles without context can serve as a description of reality in many different contexts. A simple testament to the power of these principles is that our understanding of the laws of motion and formulation of mechanics is built on symmetry in space and time. However, these types of con-

servation principles are not clear for disordered materials, where different kinds of symmetries are broken [2, 3]. The linchpin of this dissertation is to explore how to bridge the complex behaviors of different disordered systems using a single framework that is premised on avalanches as a driving mechanism for spatiotemporal complexity [4], and then to analyze the nature of those avalanches, particularly in terms of the constraints that give rise to them, which in turn informs what parameters can be tuned to extensively produce them where they do not naturally arise.

1.1.1 Spatial Complexity

In disordered systems, spatial symmetries are non-existent, and the fundamental laws which govern the structural dynamics are not easily analytically tractable due to the multivariable and combinatorial nature of components' interactions. Concrete examples of this particular aspect are nearly everywhere and tend to be intuitive. We start with an example most relevant to this thesis: windows and containers are often made from glass, which is an amorphous material with little structural clarity that would indicate the fact that it is actually flowing, just at imperceptibly slow time-scales [5][6] [7]. Unlike ordered materials such as crystals [8], arrangements between particles in a glass are heterogeneous, which gives them greater viscosity and therefore higher persistence - spatial complexity is due to particles known as "soft spots" that are more prone to moving than others. In biology, for example, the embryogenic process in organisms is considered "glassy" since tissues contain heterogeneous cell organization and motion, and it is unclear what structural variables govern the very distinct, yet deterministic cell nucleation behaviors [9]. With the rise of computational social science since the 1970s, examples in this area are aplenty: Forrester's "Urban Dynamics", which piqued Kadanoff's interest in public infrastructure is an epitome of spatial complexity in society [10]. A tangible example is in the economy, on individual level, all agents theoretically have the same goal, which is to maxi-

mize their utility function subject to the same information, and yet macroeconomic problems like unemployment arise that affect groups differently, due to unaccounted variables and "coordination" failures [11]. For all of these systems, there is clearly a need to understand a feedback mechanism between the components, that relates microscopic to macroscopic behavior.

1.1.2 Temporal Complexity

To address multivariate and combinatorial systems as mentioned in the previous section, statistical physics has traditionally been the perfect tool to relate microscopic to macroscopic dynamics. It does so by representing macroscopic states as an ensemble of many microscopic states, then writing concise canonical partition function that can generate various attributes about the system using partial differential relations between variables [12]. Even the treatment of fluctuations can be simple through the assumption of Gaussian processes and therefore, also the assumption of central limit theorem in the asymptotic regime. Unfortunately, these assumptions are invalid for disordered systems that have fallen out of equilibrium. This leads to another challenge: For a system that is not in equilibrium, it is unclear whether averaged descriptions are truly sufficient, since all "microstates" are no longer equally likely.

While most real systems, like in biological processes, are naturally out of equilibrium [13], we are mainly concerned with quenched disorder that is out of equilibrium, which can also serve as a model for other complex systems. Disorder that has fallen out of equilibrium through a quench, undergo a slow relaxation process towards its equilibrium state (albeit, unlikely that it will ever get there), also known as "aging" [14]. A key part of this process is the imprint of the system's history, which means that if t_w is the "age" of a certain system, then its dynamics will change as a function of t_w (its past events).

Here we discuss terminology that will be used throughout this thesis regarding

"aging". Glasses and relaxation phenomena are often discussed together, including in this thesis. The reason can be explained using one of the first examples in 1.1.1: When liquid undergoes a thermal quench so rapidly that it fails to crystallize, it undergoes a glass transition instead, where there is a viscous slowdown by many magnitudes. How the transition from the liquid to the glass stage occurs is still a big mystery, known as the glass transition problem, but this is an equilibrium phenomenon and therefore outside the scope of this research. Once a system is past the glass transition, it is out of equilibrium and exhibits the signatures of aging. The imprint of history is specifically evidenced through the fact that the older the glass gets, the mobility of particles, typically measured as mean squared distance, also decreases. Theoretical understanding of this relaxation is rather limited [15].

This phenomena is ubiquitous: The most obvious are in soft matter physics – polymers (which are "glassy") gradually reduce in volume as they settle into more relaxed configurations [15], the constituents of granular materials enter a jammed state without any apparent structural order, after rearrangement events triggered by an external source[16, 17], and quenched magnetic systems seem to be "frozen" into random orientations seemingly without any change in the system's symmetry for a very long time, until there is sudden change in configuration, which becomes rarer with time. Interesting biological systems are almost always far from equilibrium, in the scale of cellular processes to evolutionary dynamics [13][18][19]. Despite the qualitative and abstract commonality in all these systems, there are a lack of variables which can be used to describe them for quantitative comparison, or even distinguish them from ordered systems using a common denominator.

1.2 Practical motivation for studying far from equilibrium disordered systems

This thesis focuses more on the theoretical challenges – like finding universal features, or learning whether aging systems should be measured using averaged events (since their stasis periods are so long, anyway) or the events that punctuate the stasis (avalanches). However, there are many practical reasons for studying aging. Both theoretical and engineering challenges that ensue as a result of physical aging in glassy systems is most saliently seen in polymers, which constitute a wide breadth of materials due to their versatility. They are used in every day packaging, electronics, biosynthetic materials for implants and tissue engineering, natural gas filtration, etc – in order to get polymers to take a certain form, they are melted, molded and cooled until they resemble a solid but they are subject to the aging process that wears the very properties that are exploited in the first place [15, 20]. A suitable example for this point is that membrane technology utilize polymers for gas purification due to their porosity, but aging decreases the volume of polymers, making them denser and reducing permeability, which renders them less useful for filtration purposes [21]. Compounded with this, the history dependent behavior in aging materials creates further complications, because the time scales of the dynamics are affected by the perturbations encountered during the production process, after being molded and quenched below the glass temperature[15]. On top of all of this, how these perturbations affect the time scales vary from polymer to polymer. Therefore, it is necessary to understand the simple picture first, even to tackle the engineering problems.

Studying the actual process of physical aging is difficult precisely because it is so slow, so models that resemble aging systems combined with computationally efficient simulations that allow wider parameter explanation are valuable.

1.3 Order parameters

The central task for theorists is to find a set of organizational principles, independent of context, that can explain the behavior of multiple complex systems through their common features. This goal has somewhat of a precedence in statistical physics through the idea of "universality" which argues that a simple theoretical model can be used to capture the main dynamics of systems with different microscopic details. This is done by keeping details that matter to the dynamics from ones that do not, usually through coarse-graining – with the example that is most prominent being renormalization. Systems simplified through coarse-graining, which show similar behavior at different length scales, are considered to be in the same universality class.

Being able to group different kinds of systems is not an obvious task, since it is contingent on identifying an *order parameter* [22]. A broken symmetry (or several broken symmetries) exist for systems that are far from equilibrium and to describe them macroscopically, the order parameter is an ad-hoc variable that describes the *extent* to which the symmetry is broken. It needs to be defined, based on some coherent behavior. The choice of order parameter is crucial because not only does it affect the universality class, but also helps detect phase transitions and critical points. Along these lines, one point of contention in this research is to use a new order parameter as a way to delineate between two systems whose relaxation dynamics is often put in the same category. This research does *not* try to establish a universality class yet, but merely illustrates that a different choice of order parameter can elucidate fundamental differences in how two separate systems age due to their inherent structural differences. A "toy" model (called that cluster model, which mimics colloidal dynamics) that is purely based on this order parameter is then used to reproduce quintessential features of aging behavior, which will be discussed in great detail in later parts of this thesis.

1.4 Ising Models

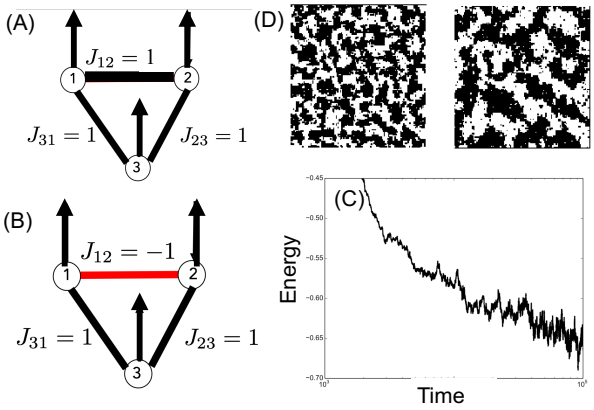

Figure 1.1: Summary of this section. On the left column, (a) depicts a ferromagnet where all bonds are the same and consequently, constraints are not complex enough to create perpetual frustration unlike (b) which shows a spin glass. In the depiction, the red bond is frustrated since it favors opposite facing means but this bond cannot be satisfied without frustrating another bond. On the right column are different visualizations of relaxation. (c) corresponds to the aging of the spin glass after a hard quench, whereas (d) shows a visual of "ordering" from the paper [23]. The blocks of homogeneous regions are known as domains, where all the spins face the same direction. In a ferromagnet, larger domains of spins facing the same direction indicates larger equilibrated regions. This is not the case for SK, since the bonds don't necessarily favor spins facing the same direction.

Toy models are supposed to represent more complicated systems, stripped of their "unnecessary" details. Examples of existing ones include Ising spin systems, graph networks, total asymmetric exclusion model, etc, which seem deceptively simple and a farcry from reality, and yet they produce rich and nontrivial behavior.

Ising spin models consist of random couplings between variable spins and are considered to be simplest representation of complex systems. The model consists of spins (s_i) with only one degree of freedom – its orientation, which can be facing up ($s_i = 1$) or down ($s_i = -1$). Spins are coupled to one another with a bond/interaction coupling, denoted as J, which can be drawn from a bimodal distribution or a Gaussian distribution. (The admixture can be used to control the "glassiness" of the model.) The Hamiltonian for an Ising spin system with N spins is the following:

$$\mathcal{H} = -\sum_{i}^{N} J_{ij} s_i s_j - H_{ext} \sum_{i} s_i \tag{1.1}$$

where h is an external field. The couplings, or bonds themselves, are obtained from either a Gaussian distribution of J,

$$P(J_{ij}) = \frac{1}{\sqrt{2\pi J^2}} \exp\{-\frac{J_{ij} - J_o^2}{2J^2}\}, \tag{1.2}$$

where $J \sim \frac{1}{N}$ or a bimodal distribution

$$P(J_{ij}) = p\delta(J_{ij} - J) + (1-p)\delta(J_{ij} + J), \tag{1.3}$$

where J is ± 1.

We primarily work with two types of spin glasses: the mean field model, known as the Sherrington Kirkpatrick (SK) spin glass, where every spin is coupled to every other spin and thus, there is no locality [24]. The second model is the nearest neighbor model on a lattice of L^d where d is the dimension, known as the Edwards-Anderson (EA) spin glass (when $d = \infty$, the EA has then reached the SK limit) [25]. Contrary to SK spin glass, the finite dimensional EA spin glass is a lattice model, where every spin only interacts with its nearest neighbors. For both of these, the admixture of ferromagnetic and antiferromagnetic spins are represented by p. When $p = 1$, the system becomes a full ferromagnet and when $p = 0$, it is an antiferromagnet.

The dynamics of these models are governed by the following: If the bond between two spins is zero, the spins will orient either way with no energy cost (ΔE). If the bond between two spins are negative, then spins need to be faced opposite directions in order to "satisfy" the bond. Lastly, if two spins are coupled by a positive bond, then the spins need to be facing the same direction in order for that bond to be

satisfied. "Frustrated" bonds are ones that are not satisfied (as illustrated in the figure), as a result of competing interactions. One can imagine the following scenario to understand how aging plays out in an Ising spin system.

For example, if there is an admixture $p = .5$ in a bond matrix in Equation 1.1, the ratio of ferromagnetic to antiferromagnetic bonds is 1 so frustration is inevitable. At a very high temperature, the spins fluctuate repeatedly, where any configuration is equally probable. However, the moment the spin glass is quenched to a very low temperature $T < T_g$, the current configuration will "freeze" in its frustrated state, and will minimize frustrated bonds very slowly during its relaxation process. The geometry and growth of interface between the domains is also integrated into the real-space droplet model, and studied to better understand aging and its resemblance to coarsening, which will be discussed in greater detail in 2 and other parts of this thesis.

1.5 Energy landscapes

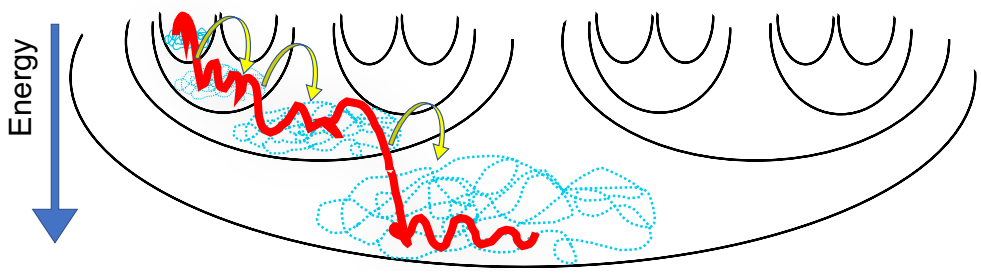

Figure 1.2: Hierarchical energy landscape. An example is drawn of a hierarchical energy landscape with a black outline. Each of the basins/valleys represent an the same energy "level" or "tier" within the hierarchy, although there may be differences in the microscopic arrangements within the system (similar to the equilibrium macroscopic-microscopic relations). However, the difference in the out of equilibrium regime is indicated by the yellow arrows – with large enough fluctuations, the system will be able to escape from its current basin to the next "lower tier" – i.e the next marginally more stable state.

Glassy materials like amorphous fluids [14], jammed grains [26, 17], colloids [27, 7], disordered magnets [28, 29], or entangled polymers[30], all face frustration while relaxing their free energy. Due to competing variables exerting geometric or energetic constraints on each other, a complex, multimodal landscape is imposed on the space of all possible configurations. A universal framework of how a system traverses its landscape can shed light the organizational principles that give rise to different phases of behavior[2, 3]. In order to understand these principles, it is necessary to understand the basics first: Namely, what are the different states (configurations) of the system, and what do the transitions between the states look like? Thermodynamically, "states" refer to energetic states – one can write an energy function of a configuration and determine that the most thermodynamically stable state is the state with the lowest energy, and thus preferred at $T \to 0$. Higher energy values indicate higher "frustration" in the system. Thus, the surface of an energy landscape is a schematic of the "frustratedness" where different energetic states are depicted by different basins (or valleys, local minima, etc), and the transitions between states are represented by energetic or entropic barriers that appear as ridges between the two different basins.

In the 1960s, to further understand the puzzling nature of viscous flow in glass, this energy landscape scheme was proposed by Goldstein as an alternative to existing theories[31]. The scheme developed by Goldstein was simple – the potential energy function encapsulates both the transport and configuration of a system, so the state of glass can be seen as any point along the potential energy surface, that would also need to account for the temperature. At zero temperature, the glass does not have movement and would therefore be stuck in a configuration that is considered a potential minima, although this is not necessarily the optimal minimum. In order to change configurations, the molecules will need some kind of activation energy that will mobilize them and facilitate a rearrangement, which will land them in a new minima.

To describe organizational principles of glass, potential barriers are used to describe the transitions while the basins are used to describe the configurations. To probe the inherent structure of the landscape, one can imagine the representative state point on the potential energy landscape moving as a function of temperature. That said, the most "naive" landscape consists of a sequence of minima and random barrier heights, termed random energy fields (R.E.F) [7]. The conjectures surrounding the structure of basins have evolved since – rather than being random, barriers are structurally organized in ways that are distinct to certain materials and systems.

This construction is easily translatable as energy landscapes are widely used across different fields [32]. For example, in biology, Waddington epigenetic landscapes represent cell differentiation as a point rolling through a surface where each valley represents a cellular state [33, 34], fitness landscapes separate valleys based on mutations [35], and adaptive evolution can be studied through tunable landscape like the NK model in which the effect of agent on the landscape structure itself can be studied [18]. In engineering, the design of amorphous materials requires studying how interatomic potential functions give rise to particular landscape attributes [36], which directly affect their dynamics. On the computational side of things, lossy landscapes in deep learning represent the a high dimensional cost function, similar to parameter spaces in optimization problems [37]. To fully understand this range of systems, there are two main and intertwined challenges, concerning the energy landscape – (1) What is the structure of the barriers? To answer questions that reveal universal patterns in the structural features of the landscape, it is also necessary to be able to sample enough of the space. This becomes a challenge in multivariate systems with a large parameter space, which leads to another related aspect – (2) How can one sample high dimensional complex energy landscapes in a way that is computationally efficient?

Specific physical systems correspond to specific landscapes (the ones representing proteins come in many forms such a funnel or a golf course but ultimately have one

clear minima, whereas the SK spin glass has a hierarchically organized landscape, for example). Therefore, to understand phenomena in disordered system, it is best to start with a system that is versatile and easily generalizable, which is another advantage of using the Ising spin glass models described in 1.1.

1.5.1 Mean Field Theory

What does it mean to "understand" the full energy landscape picture? The mean field spin glass is a perfect example of a system whose energy landscape structure is understood relatively thoroughly thanks to analytical calculations performed by Giorgio Parisi, leading to replica theory for the SK model [38, 39]. The crux of his calculations was that probability distribution of "pure states" was non-trivial - rather, it seemed to demonstrate ultrametric structure. The physical meaning of this is that the free energy landscape has a hierarchical organization, where the states themselves are self-similar [40]. However, whether these characteristics can be applied to other glasses has been unclear until more recently with landscapes of jamming transitions in structural glasses showing ultrametric structure [41]. From a plethora of literature, it is clear that one possible way to understand the glassy structure is through the framework of the mean field model.

Showing that mean field theoretic tools can be used for structural glasses as well, means that the energy landscape in structural glasses initially has a random first order transition (a landscape that consists of a featureless basin and large barriers) but through the Gardner transition, the basins begin to have a fractal structure, or a hierarchy of sub-basins [42, 7]. It is said that after the Gardner transition, the structural glass has properties akin to the Sherrington-Kirkpatrick model (SK). Having a structure that resembles the mean field model means that it can be subject to same analytical tools.

In terms of the aging of glassy systems, there are several implications of using

mean field: First, the physical interpretation is that as a system ages, it is continuously descending down an energy landscape (which has exponentially many states) [23]. In terms of observables, measurements require using averaged statistics: For instance: one can measure a correlation function between the variables as they age, where $C(t, t_w) = \langle S(t)S(t_w)\rangle - \langle S(t)\rangle\langle S(t_w)\rangle$ where S denotes an observable, and the $<>$ indicates both a thermal and disordered (different bond realizations) average over an ensemble. Similarly, the susceptibility, $\chi(t, t_w)$ is based on an **averaged** response function $R(t, t_w)$ to a discretized change in local field, since it calculated by $\int_{t_w}^{t} dt' R(t, t')$, so it is integrating information over time.

In this thesis, it is argued that this mean field theory approach ends up throwing out important information about the system – mainly its avalanches (i.e all forms of activated dynamics), as elaborated in the next section.

1.6 Avalanches

So far, it has been established that mean field theory is considered convenient and aspirational in the disordered systems community. However, the fact that it involves averaging information over time, means that it can also lose information about rare "activated" events – also referred to avalanches, record events, quakes, etc (in this work, all of these terms are interchangeable). Thus, one prominent theme in my thesis is comparing the description of aging using the rare events, rather than averaged ones (mean field). Another overarching theme is investigating the role of these avalanches in aging processes, and the generation of avalanches in general.

Why the emphasis on avalanches? These events are of interest because there is evidence that intermittent avalanches create substantial structural changes in a system. To paraphrase a quote in [4], avalanches are the source of spatiotemporal complexity, throughout nature and natural history. For example, in biological evolution, though

contentious, the theory of "punctuated equilibrium" argues that evolutionary periods are mostly static with intermittent bursts of changes [43] – the sudden introduction of a new phenotype will allow species to exploit new features of an environment, and thus momentarily changes the evolutionary dynamics. Along the same lines, mass extinctions create substantive changes to evolutionary dynamics and ecology for [44]. Earthquake faults are another common example of such bursty dynamics [45, 46, 47], among depinning transitions in charge density waves [48], superconducting vortices [49], granular media [50], and even neuronal dynamics in the brain [51]. Although of course, these examples are driven where "aging" is a naturally occurring process, but the effect of avalanches are similar in both.

Between the "quasi-equilibrium" or metastable states, aging progresses with large intermittent fluctuations. The significance of these intermittent events during the aging process were not "obvious" previously, but became salient experimentally through aging colloids, where time resolved correlation showed bursts of long range correlations corresponding intermittent events [52]. Such rare intermittent events are key to evolving the system, since it is only during long-range rearrangements that any substantial changes in the system occur – for instance, this is essentially the difference between cage rattling and cage breaking events in jammed glasses [53], where the former is only ballistic motion among a smaller group of particles, and the latter creates enough motion to completely change neighborhoods.

1.6.1 Record Statistics

Even if the aging and driven processes do not originate from the same mechanism by nature, several things are clear: the record fluctuations are what break time reversal symmetry; this means that they serve the role as the system's "internal clock" since they determine the time-scales of different configuration states. If that is the case, then what if these were the only events that "mattered" in the relaxation process?

This assumption is what underlies the coarse-grained description of aging processes, known as record dynamics [54, 55, 56, 57, 58, 59]. Under this framework, a system that is undergoing the relaxation process is seen as ultimately tumbling down a series of metastable states that are hierarchically arranged, within its complex energy landscape. A record fluctuation is therefore supposed to be an indication of having overcome an energetic barrier and tumbling onto the next more marginally stable metastable state – or in other words, the "next step" down the hierarchy of basins (see Figure 1.2). The rate $\lambda(t)$ at which such record fluctuations, also known as quakes, occur, decelerates with time as $1/t$. The expected number of events in a time interval $[t, t_w]$ is therefore,

$$\langle n(t, t_w) \rangle \propto \int_{t_w}^{t} \lambda(t')dt' \propto ln(\frac{t}{t_w}) \tag{1.4}$$

. Given the "fixed" average number of events per logarithmic time, aging is a log-Poisson process. Studies in the past have shown that these statistics are in agreement with previous experimental studies on jamming colloids [57].

Indeed, there are older models that are based on activated process, also known as "activated barrier hopping". In the trap model [60], for example, an "energy landscape" is composed of a surface with wells (representing the minima) with depths that correspond to the activation energy, or energy required to overcome the trap. When a system is aging, it will fall down a series of wells as it does a random walk on the landscape. Every time the system falls into well (a trap), it will take τ time to escape the trap. In this case, $\tau(x) = \exp(\beta E_x)$ where E is power law distributed. While the trap model may have successfully schematized aging, the fundamental difference between the RD framework and the trap model is that RD has memory, which is more true to the history dependent behavior in aging – valleys are defined contingent on previous valleys that have been encountered. On the contrary, the trap

model is memoryless and treats aging as a renewal process. Therefore, this activated model is different from previous ones because it operates on completely different assumptions.

1.6.2 Hysteresis

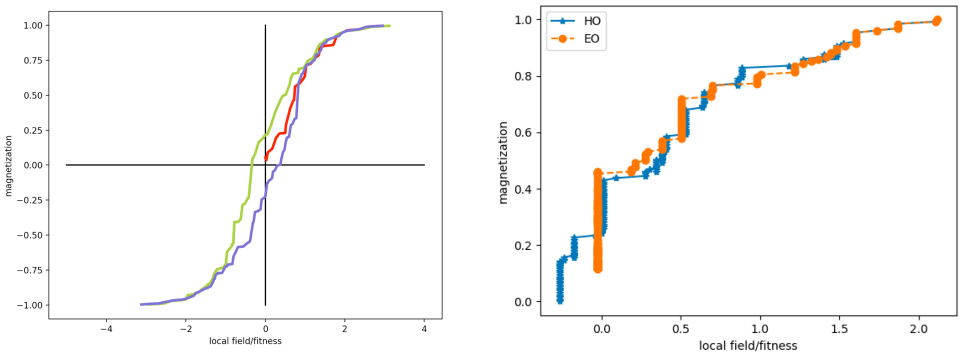

Figure 1.3: Example of a hysteresis loop. On the left is a typical hysteresis loop, where a spin glass starts at a magnetization of zero, and is exposed to an external magnetic field that gradually increases until the system is fully magnetization, but once the direction of the field is reversed, there is a lag time between the system's magnetization matching the external field. The right column shows a closer look of the hysteresis loop in order to discern the avalanches, which occur every time there is a change in magnetization. It is clear that avalanches grow in size closer to a coercive field of zero.

There are many questions surrounding critical avalanches, independent of aging: How does a system's history affect its generated avalanches? What are the parameters within the dynamics that determine the scale of an avalanche? How do correlations build during an avalanche, if any?

It is much easier and accessible to approach these questions through driven disorder, rather than aging processes due to the inconvenient time-scale of the latter. For driven disorder, hysteresis, which has been most widely used in magnetic systems, proves to be an appropriate tool since it has a couple of the same features as aging glasses like being in a nonequilibrium regime, having history dependence and avalanches.

Hysteresis is a memory effect - more specifically, it describes the phenomenon of when a system is subjected to a changing external force but the system's history dependence makes it react to the varying external force with a lag time [12]. The "sensitivity" of certain materials to the applied force varies - some will "crackle" or display bursty dynamics whereas others will be robust to small values of the external force f until a threshold is reached, which will the depin the material [61], exhibiting a first order phase transition. This first order phase transition makes hysteresis a useful phenomenon to exploit for materials with switches.

When a ferromagnet is exposed to an external magnetic field H_{ext}, and that magnetic field is slowly ramped up, then the ferromagnet will yield – i.e individual spins will align with the external field. However, when the external magnetic field is ramped down to return to $H_{ext} = 0$, the spins will take a longer time to recover their order due to new barrier formations, which means that even when $H_{ext} = 0$, there will be remanent magnetization. What is especially interesting and relevant to this research is something called Barkhausen noise that was observed in both ferromagnets and the SK spin glass [62, 63, 64]. Here, as the magnetic field is ramped, it "depins" domain walls, leading to clusters of spin flips that successively lead to pinned configurations, until there is stability. The sequence of spin flip (the avalanches) in Barkhausen noise also happen to exhibit a power spectra with an exponential fall off [65] . The fact that the system can do this without any parameter tuning, was considered to be a sign of self organized criticality (SOC).

For the SK model in particular, the wide range of avalanche sizes has been exploited to help find lower energy configurations by overcoming large barriers (as opposed to Monte Carlo or gradient descent) through an algorithm called hysteretic optimization (HO) [66, 67]. Here, an external magnetic field is used to add Barkhausen noise to the system, which gives the spin an energetic "kick" to rearrange into substantially different configurations that can help overcome energetic barriers. If a gradient

descent method were used, the system would remain trapped in a local minimum. When the same protocol is performed on the EA model, for example, the avalanche spectrum remains subextensive, which means that one cannot use HO for sparse systems. This occurs because correlated behavior is only confined to neighbors, and in order for there to be critical avalanches, there needs to be long-range correlations.

Another broad theme of my research is to understand whether critical behavior can be induced in sparse systems through driving methods that deviate from traditional hysteresis. While there is an understanding that the all-to-all connectedness in the SK model helps it have long-range correlations, an external magnetic field introduces more bias into the correlated behavior. To understand how this leads to criticality, one approach is to study the state that immediately precedes an avalanche, called the marginally stable state. What does the marginally state of the SK model reveal about how it should be perturbed in order to get critical avalanches? What would one have to do to equally perturb the marginal stable configuration in EA, and get critical avalanches?

1.7 If a spin glass avalanches, does a traveling salesman see it?

Optimization theory is naturally related to the topic of spin glasses, which is a NP-hard problem, which is a problem for which solutions cannot be verified deterministically. After all, just as avalanches help an aging glass move along meta-stable states, they can also be used to explore better solutions in a combinatorial optimization problem provided that the avalanches trigger the right correlations to facilitate "learning" the landscape.

In the prior section, hysteretic optimization (HO) was mentioned as just one heuristic to explore spin configurations in the SK spin glass [67]. This heuristic

operates on criticality – avalanches of a broad size distribution means that more distinct configurations are explored, which makes it easier for the system to escape local minima [68, 69]. Of course, there is no guarantee that the solution will be optimized. Thus far, there is no mechanism that explains why a critical state per se would have any connection to finding necessarily *better* ground states, but it does at least provide better opportunity. However, there is a collection of literature that does define the critical state as being optimal for information processing in computation and even the brain. In the classic Langton paper "Computation at the edge of chaos", criticality is defined as being in the border between order and disorder, which is supposed to allow optimal trade-off between retaining memory (the right information for learning by remaining "ordered") and learning new information (through disorder) [70]. The importance of criticality has even shown in "plastic adaptation", a process that facilitates learning[71, 72].

The very last and (incomplete) part of my research investigates whether critical fluctuations are enough to improve an optimization algorithm, and tries to understand the feedback mechanism that helps coordinate the information processing.

1.8 Outline

So far, I have summarized the requisite concepts that led to my research projects.

Chapters 2 and 3 are anchored in record dynamics, as discussed in 1.6.1 part of the introduction. Collectively, these chapters establish that RD is a sufficient description of aging, because unlike previous work (to our knowledge), it integrates intermittent events to create a coarse-graining framework (described in the computational methods section) and is able to discern between systems that were placed into the same category, or "universality class", that we now know is not actually the case. If RD truly captures the "essence" of aging, then a model that embodies purely RD princi-

ples (everything else is coarse grained out) should be able to replicate the anomalous signatures of aging, such as memory and rejuvenation. The breakdown: Chapter 2 therefore describes one of my first projects, which uses "aging" as a protocol to probe energy landscapes and finds using the RD based order parameter that "true" aging is different from coarsening. Chapter 3 shows that a very minimal model, named the cluster model, that is based purely on record dynamics phenomenology is able to reproduce the behavior of aging systems (memory and rejuvenation) and how these phenomena can be explained by the hierarchical energy landscape.

Chapter 4 discusses how the mutual frustration between marginally stable spins leads to strong correlation structure that causes avalanches in the mean field model. This inspires us to look at three different driving methods that change the interactions of marginally stable spins to build a correlation structure in the real space EA model. We compare the resulting avalanche distributions, and then find the best parameters that would facilitate long-range correlations in the EA model.

In Chapter 5, I summarize work that is built on analysis performed in Chapter 4 and explore the implications of this on an NP-hard problem.

Chapter 6 concludes my thesis with a discussion.

Chapter 2

Valleys in aging and coarsening processes

2.1 Summary

Referring to the definition in section 1.1.2, "aging" refers to slow relaxation towards the equilibrium state, and the literature which describes this process has many subtleties. Through a coarsening paradigm, aging is depicted as a gradual ordering of the system; the ordering is measured through a correlation length scale $L(t)$, which involves taking coarse-grained measurements of correlated activity over time, [73, 23, 74]. While there are different classes of coarsening, to say that aging and coarsening are the same is misleading – In the literature, the ferromagnetic coarsening picture is used to create generalized scaling assumptions on spin glass aging, which is problematic because their dynamics are fundamentally different. The crux of the problem is rather simple – aging is only one kind of coarsening and it applies to disordered systems (like glasses) only, not ferromagnets. To avoid such confusion, we propose using a new order parameter entirely based on record dynamics (RD) that directly elicits the barrier structure in the landscape to interpolate between glassy and ferromagnetic

behaviors. This method ends up having two advantages - first; it clearly interpolates between the logarithmic aging in glasses in comparison to the linear aging in a ferromagnet (the range between a full ferromagnet and a full spin glass have not been explored before, except in [75] where the critical exponents in the growing correlation length was used to interpolate between the glassy and ferromagnetic regime). The distinguishing factor in our study is that RD is based on intermittent (rare) events, which was experimentally noted to be a signature of aging [52]. In both of classes of Ising models that we use - the real-space Edwards Anderson spin glass and mean field Sherrington Kirkpatrick spin glass - we are able to find a critical point that delineates between ferromagnetic and glassy regime based on how barriers scale with the ordering length scale.

This section of the thesis is based on the paper "Analysis of landscape hierarchy during coarsening and aging in Ising spin glasses" in: Phys. Rev. B 103.2 (2021), pp. 1–8, authored by Stefan Boettcher and Mahajabin Rahman. The EA simulations were performed by Stefan, and SK simulations were performed by Mahajabin.

2.2 Introduction

In previous literature, aging has been described by a process in which systems gradually equilibrate through coarsening [23], which is synonymous to the domain growth. As part of the ordering process, regions of the system begin to locally equilibrate into homogenous clusters known as domains. Then, such domains begin to "compete" with one another, until smaller domains merge with larger ones, eventually leading to global equilibration [76]. Two aspects of coarsening are emphasized: (1) its representation of correlated and thus, coherent behavior, of the spins as they move an interface boundary, and (2) because moving an interface boundary has an energy cost ΔE, the rate at which the length scale of the average domain grows can have depen-

dence on the free energy barriers [77]. The growing correlation length measures how close a system is to its equilibrium state. As it approaches there, it does not reach a stationary state but merely arrives at a state of detailed balance. This indicates a lack of bias in terms of fluctuation probability, such that the system appears reversible instead of "flowing" towards a certain configuration. At equilibrium, the notion of a "dynamic length scale" exists to describe macroscopic correlated behavior in the form of $C_{AB}(r_1, r_2, t) = \langle A(r_1, 0)B(r_2, t)\rangle$ where A and B denote some observable, such as spin orientation, for example, and r_i indicates either location in real space or an index at a given time, t [78]. Although equilibrium systems are not static, the canonical ensemble average is able to capture correlations that are conserved from one configuration to another. This equilibrium concept is then extended to out of equilibrium systems, through the idea that while a system equilibrates, there is also an *increasing* correlation length [73]. This series of events can easily be visualized in a ferromagnet: When quenched from a high temperature $T > T_g$, to a low temperature $T < T_g$, spins in a ferromagnet appear to be in a kinetic arrest due to their mutual frustration. Very slowly, they will re-orient themselves into small clusters (domains) where they are all facing the same direction, until eventually a cluster has expanded throughout the system, such that all spins are correlated to one another and always facing in the same direction whether it is up or down. In comparison to this, coarsening is rather difficult to visualize in spin glasses since clusters of uniformly oriented spins lose significance when the interaction energy J has an admixture $p \neq 0$. However, even though domains in spin glasses cannot be pictured in the same way they can in ferromagnets, the representation of a domain through a correlation length, must still exist in spin glasses. The extension of ferromagnetic coarsening to generic aging phenomena is the reason much of the literature leads to the impression that relaxation via coarsening in a ferromagnet and glassy aging are similar [79, 74, 23]. We already know in contrast to the hierarchical, multimodal energy landscape of a glass, that of

a ferromagnet is smooth, so it is unclear that they should coarsen similarly.

There are different kinds of coarsening, expressed through a simple calculation where the characteristic size of locally equilibrated domains generally scale as one of the following:

$$L(t) \sim t^{z(T)n} \tag{2.1}$$

$$L(t) \sim z(T)\ln(t) \tag{2.2}$$

where z is pre-factor that is temperature dependent contingent on the system in question [80], in order to account for the difficulty in overcoming entropic barriers, and n differentiates between universality classes for fundamentally different growth patterns based on interfacial dynamics [81].

Related to equation 2.1, there are two prevalent types of coarsening in nature, for which there are designated universality classes that indicate fundamental physical difference: $n = \frac{1}{3}$ describes a growth called Lifshitz-Slyozov, where interface dynamics lead to phase separation, also known as spinodal decomposition, a mechanism that forms patterns in polymer blends [82, 83], surface waves [84], and dendritic growth [71]. Through all of these processes, the system's order parameter is conserved [76]. Recall from section 1, the order parameter is an the ad-hoc variable that discerns the "brokenness" of symmetry, which in this case is the number of molecules of each subspecies/phase. In spinodal decomposition, a conserved order parameter means that different species are spatially separated, the number of molecules of each type remains the same. On the other hand, $n = \frac{1}{2}$ describes the Lifshitz-Allen-Cahn growth where the domain expansion is curvature driven, and the order parameter is not conserved i.e the phase order kinetics changes the symmetry breaking. This type of growth describes the grain growth in metals, ordered arrangement of binary alloys, coarsening of a foam, for example, where surface tension generates curvature

driven growth of the bubbles. The point of these example is to illustrate that the differences in the universality classes do happen to make a difference and can have tangible impacts in real life – in fact, space shuttle experiments were conducted just to understand the coarsening of metal alloys, which can be used for designer materials that constitute everyday technology such as automobiles and aircraft [85].

Equation 2.2 describes logarithmic coarsening where the free energy barrier itself scales with the length, such that the rate of interface growth (dL/dt) follows Arrhenius behavior $dL/dt = z_0 \exp(\frac{E_B}{k_B T})$. As the correlation length grows, it becomes increasing more difficult for separate domains to "merge" because the energy cost (ΔE) to initially flip spins along either boundary becomes higher, leading to slower growth. This class of growth is more relevant to this work, as it pertains to systems with randomly imposed disorder such as random field Ising magnets or spin glasses. However, as stated explicitly in [81], universality classes are subtle. These are not the only coarsening patterns possible, so physicists are always trying to delineate details within them [86].

Unlike the established growth classes which have been mentioned, which use order parameters based on "real space" - whether it is magnetization or number of molecules, the order parameter introduced in this paper uses the trajectory through the energy landscape instead of the physical "space". This new order parameter is based on a phenomenological description of aging called record dynamics, cursorily introduced in 1.6.1. It is almost natural to use record dynamics as a framework to choose an order parameter from, for the following simple reason: non-equilibrium systems have a clock because they change over time, whereas equilibrium systems do not. Therefore, if record fluctuations act as a system's "internal clock", then the number of record-size fluctuations that have facilitated the system's tumbling down n_v valleys, is a reflection of how much time has elapsed, a measurement that is only meaningful in systems that age. We are further encouraged to use the RD framework

because previous experimental results in [57] with jammed colloids fit the RD description, discussed more thoroughly in 1.6.1. Now, the RD-borne order parameter, the number of valleys the spin glass has passed through (n_v), which is described in further detail in the Methods (2.3) is put to test, by discerning ferromagnetic from spin glass behavior. While it may be a matter of semantics, if being able to delineate between different dynamics is a meaningful goal, then it can be argued that understanding aging as as coarsening can be misleading for several reasons. The very simplest argument is that while there are different classes for coarsening, there are not different classes for aging – if aging is a particular instance of coarsening, then it would be incorrect to say that all coarsening processes are also aging, which ends up putting ferromagnetic and glassy relaxation dynamics in the same category [79, 74, 23]. For instance, the coarsening picture is used to arrive at the ferromagnetic measurement $L(t, tw) \sim \frac{t}{t_w}$ in [23] which is then generalized to all of aging since it reflects history dependence, but also depicts spin glasses and ferromagnets similarly. As discussed before in this section, and in [81], the two systems have fundamentally different dynamics as they coarsen.

Our RD-based order parameter, n_v, is more closely tied to the barrier structure of the energy landscape, and thus the coarsening discussion on systems whose correlation length scales increase with barrier sizes. After all, the structure of landscapes hugely affects the dynamics of the systems evolving through them, as more complex energy landscapes can possess a myriad of metastable states to temporarily or permanently trap any dynamic process, making periods of relaxation appear kinetically arrested. Glassy and otherwise homogeneous systems such as a ferromagnet distinguish themselves in the manner that fluctuations affect their relaxation dynamics. In the latter, barriers are comparably low and remain invariant independent of the depth within the landscape and, thus, of the age of the process. Fewer events, like the evaporation of a domain in coarsening, happen not because individual events become

so much harder, but rather because fewer events can happen with fewer domains left. Larger domains may take a little more time to evaporate, as meandering interfaces need to find each other and collide, but such an entropy barrier does not dominate the otherwise domain-size independent energetic barriers [81]. Yet, fluctuations of any size can bring those interfaces together.

In the glassy system, however, it is the barrier height growing with domain size that decelerates the event-rate. Although many domains remain available even after a long aging time, few muster the chance fluctuation required to disintegrate or shrink the domain. In a landscape with those barriers, ordinary fluctuations become ineffective to drive the relaxation process. They merely "rattle" the system in increasingly longer quasi-equilibrium interludes. Only rare, extraordinary large, in fact, record-size fluctuations manage to scale such barriers to expel excess heat, advance the relaxation, and grow domain size, minutely. Record dynamics is inspired by these very features which are shared across a wide breadth of disordered systems.

In this work, we use a class of Ising spin models with the Hamiltonian described in equation 1.3, and vary the admixiture p from the glassy state (at $p = .5$), to wherever clear ferromagnetic behavior emerges in order to interpolate where the landscape structure undergoes a transition from the glassy to ferromagnetic regime. We only employ record dynamics after using the "aging" protocol as a diagnostic tool, since variations in temperature can be used to take a full measure of landscapes. At high temperature correspondingly higher echelons in energy get explored, while annealing or quenching is used to trace out a descent through the landscape toward configurations of lower energy. A conceptually simple protocol consists of preparing a system at a high temperature, where it equilibrates easily, and then instantaneously quenching it down to a fixed, low temperature, to explore how it relaxes toward equilibrium thereafter. Such an "aging" protocol when applied to systems in a complex energy landscape, elicits quite subtle relaxation behaviors which keep the system far from a

new equilibrium for very long times. Anomalously slow relaxation and full aging in a complex landscape ensues when downward paths are obstructed by barriers, energetic or entropic, that trap the system in neighborhoods with many local minima.

Our findings confirm that while coarsening is only a specific instance of aging, aging does not indicate coarsening. The accumulation of record events grows logarithmically with time in the glassy regime for both the Sherrington-Kirkpatrick (mean-field) and Edwards-Anderson spin glass, with a sharp transition at a specific admixture into the ferromagnetic regime where such activations saturate quickly. While the test itself is incredibly simple, the implication of these being separate is that there are intrinsic differences in the structure of the energy landscapes, therefore elucidating deeper insight into the relationship between landscape morphology and aging dynamics.

2.3 Computational Methods

2.3.1 Simulation of quenches

The distinction between slow relaxation in glassy versus homogeneous systems is succinctly analyzed in the simplest conceivable protocol of a hard quench from an easily equilibrated high-temperature state into an ordered phase, whether glassy or ferromagnetic, crossing a phase transition in the process. Such a pure aging protocol has been studied extensively in the last 40 years [23, 20] In this process, the system is thrown far out of equilibrium, left with an enormous amount of excess heat to be released to the bath to be able to descent deeper into its energy landscape to reach states with the appropriate energy.

To facilitate such a quench for the family of Ising spin models considered in our study, for each instance at time $t = 0$, we initiate with randomly assigned spins, either $\sigma_i = \pm 1$, which corresponds to $T = \infty$, and run the simulation for $t > 0$ at a low,

finite temperature. For the family of mean field models, we only vary the admixture of ferromagnetic bonds minutely, so that the transition temperature does not deviate much from that of SK, which is known to be $T_c = J_0/k_B$ where $k_B = 1$ [24]. Here, we also quench to $T_q = 0.7J_0$ throughout.

We use the Monte Carlo Metropolis Hastings method to evolve the spin glass through the quench. In each "step", a spin is chosen to flip by random and this move is readily accepted if the cost of flipping the spin is negative. If not, then the move is accepted only with a probability of $P = \exp \frac{-\Delta E}{k_B T_q}$. In our simulations, the time is measured in sweeps, which is equivalent to N steps with N being the system size. One run generates a time trace, which is coarse-grained based on record fluctuations, a procedure which is described in detail below. For each value of admixture p in our investigation, we generate over 10^4 runs for at least 10^4 realizations, and average over the coarse-grained statistics.

2.3.2 Detecting records and introducing the RD order parameter

To use the RD description, it is necessary to monitor the internal energy of the entire spin system through its energy trajectory, also referred to here as a "time trace" along the landscape, after the hard quench. Since the system is expelling energy into some "bath" to relax, on average, the energy gradually decreases via localized, intermittent events which can then be captured by the coarse-graining framework inspired by RD. The very general idea is to have the time-trace coarse-grained into valleys (marked with E in the Figure 2.1) and barriers (marked with B in the same figure), to mark local minima and barrier crossings, respectively. While there are bound to be numerous barrier crossings particularly in landscape that is already rugged, this procedure only retains those rare crossings that correspond to a record fluctuation that has enabled the system to tumble into the next marginally more stable metastable

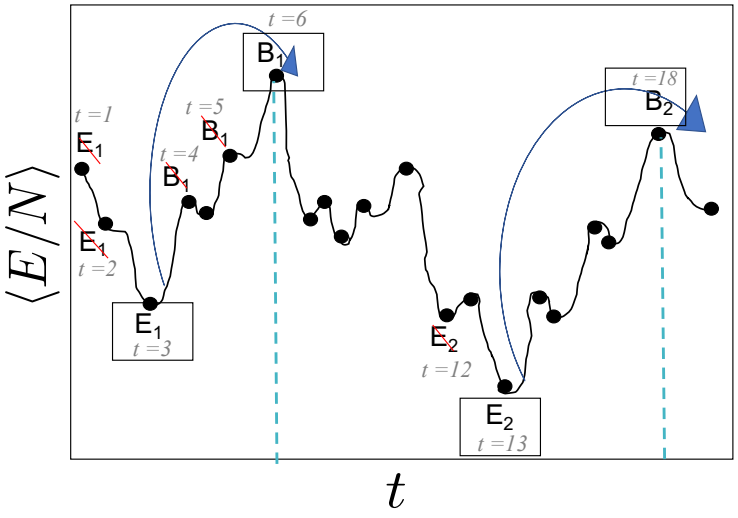

Figure 2.1: Illustration of the definition of valleys. The trace through an energy landscape produces a time sequence of energy records (E_i) and of barrier records (B_i), relative to the most recent "E_i". Only the highest and lowest records of the "Ei"and "Bj"are kept to give a strictly alternating sequence "... $E_1B_1E_2B_2$ ...." Then, any sequence "$B_iE_iB_{i+1}$ " demarcates a valley (vertical lines).

state. Discarding the rest of the information, this method is able to keep record of metastable states the system has evolved through during its descent into *distinct* "tiers" of the landscape hierarchy, as depicted in the Figure 1.2. These distinct states can be considered as macroscopic descriptions that represent ensembles of configurations where dynamics occur in homogeneous time-scales, pictorially encompassed in a single valley. Therefore, the RD-based order parameter is the number of valleys encountered n_v up to the current time (t), as it also reflects the number of record events that need to have happened in order to get to a certain local minimum. The following are the set of rules of coarse-graining the time-traces.

As mentioned before, the time trace is simply the energy value of the entire spin glass system $E(t)$ as a function of the time, as depicted in the Figure 2.1. With every accepted move by the Monte Carlo algorithm, there is clearly a new energy value. To implement this as an algorithm, it is easiest to think of this protocol in terms of simultaneously identifying pairs of energies – the lowest and highest, signifying the most extreme fluctuations. As new energy values are generated during the dynamics,

the lowest instantaneous energy ($E(t)$) that is encountered up until time (t) is marked with an "E_i" where i marks the valley index, and the highest instantaneous energy, *relative* to E_i is marked with B_i. At the very beginning of the time trace, we seek out E_1 and B_1, to demonstrate.

Immediately after the quench, the first spin flip generates E_1 since that is the only data point we have, and now we need a peak to see an activation in the energy. However, for as long as the energy decreases with more spin flip dynamics, this E_1 is repeatedly replaced with subsequent energies that are lower, such that the system only has memory of the last minimum. To permanently "lock" E_1 in place, there are two criteria: (1) the barrier height, which is the difference between the most recent E_i (E_1, in this example), and the current energy E_t needs to be the highest difference encountered, and (2) after the peak is chosen, there is an energy, after that peak, that is less than the previous $E_{\min}$, to mark the beginning of the succeeding record fluctuation. In summary, assuming the very beginning of the procedure, there must be a marking of "$E_1B_1E_2$" with the last E_2 being tentative, and it must be true that $E_2 < E_1$. E_2 then gets locked in place in the same way as E_1 and B_1. Ultimately, there should be a series in the form of $E_1B_1E_2B_2...E_nB_n$ as shown in Figure 2.1. The main observable here, n_v, or the number of valleys, is equivalent to n – the pairs of E_iB_i.

2.4 Numerical results

The results are presented for a class of Ising spin models, that include the Edwards Anderson spin glass on a cubic lattice, and the Sherrington-Kirkpatrick (mean-field) model as discussed in section 1.1. Both models are investigated, as conclusions about one cannot be drawn to the other – the flipping of domains and meandering interfaces can be visualized in the cubic EA spin glass, but not the SK model since it lacks

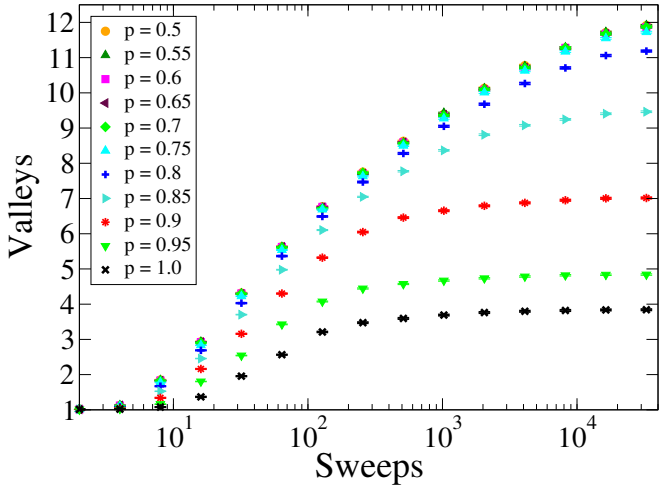

Figure 2.2: Average number of valleys in EA, as defined in Fig.2.1, that are traversed with time after a quench to $T = 0.7J_0$ in a $L^d = 16^3$ spin glass with a fraction p of ferromagnetic bonds and $1 - p$ anti-ferromagnetic bonds. For $p \leq 0.75$, the generation of valleys evolves essentially independent of p, while for a larger admixture of ferromagnetic bonds valley generation progresses to cease ever more rapidly and the number of valleys reached plateaus.

locality. Additionally, it is clear what a homogeneous ferromagnet is in both the finite and infinite dimensional cases. In both EA and SK, the admixture $p = 1.0$ by definition creates a ferromagnet, but it is unclear how many antiferromagnetic bonds can be in the mixture for the system to still maintain ferromagnetic behavior. Hence, we analyze a range to interpolate a transition point.

2.4.1 Edwards Anderson Spin Glass

Applying the measure of a valley number defined in Sec.2.3.2 to the cubic Edwards Anderson model provides a notable distinction between glassy and homogeneous coarsening behavior, as Fig. 2.2 shows. For all $p < p_c \approx 0.77$, the critical threshold found in Ref. [60], we find that the valley count progresses logarithmically in time (in fact, like the root of that logarithm [87], consistent with Eq. (1.4). For larger values of p, the valley count slows ever more significantly to eventually plateau at a finite value, ap-

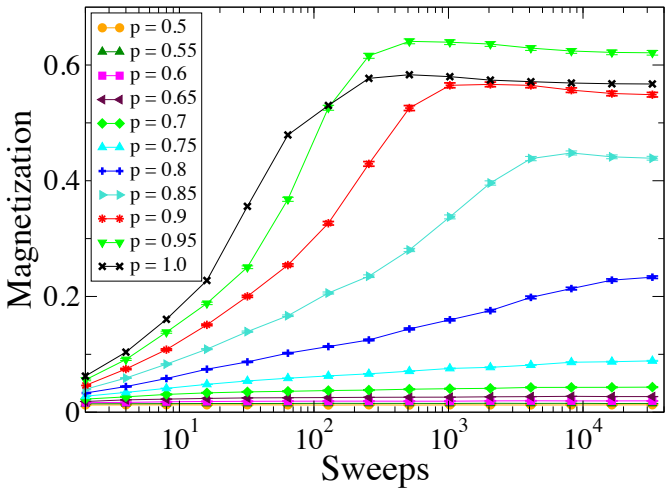

Figure 2.3: Average magnetization per spin, $\langle m \rangle$, observed with time after a quench in EA during the ensuing aging process, as described in Fig. 2.2. Like there, systems with $p \leq 0.75$ behave glassy in a p-independent manner with little discernible magnetic ordering, while the more ferromagnetic systems become increasingly more ordered.

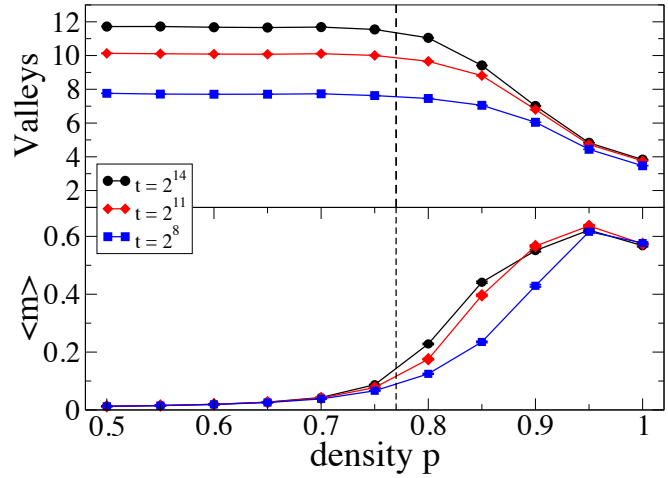

Figure 2.4: Finite-time snapshots of the numbers of valleys generated (top) and the corresponding magnetization per spin, $\langle m \rangle$ (bottom), in EA, as a function of ferromagnetic bond fraction p for three different moments in time, taken from the data at $T = 0.7J_0$ shown in Fig. 2.2 and Fig. 2.3, respectively. The vertical line at $p_c = 0.77$ indicates the zero-temperature transition found in Ref.[60] between a spin-glass and a ferromagnetic phase.

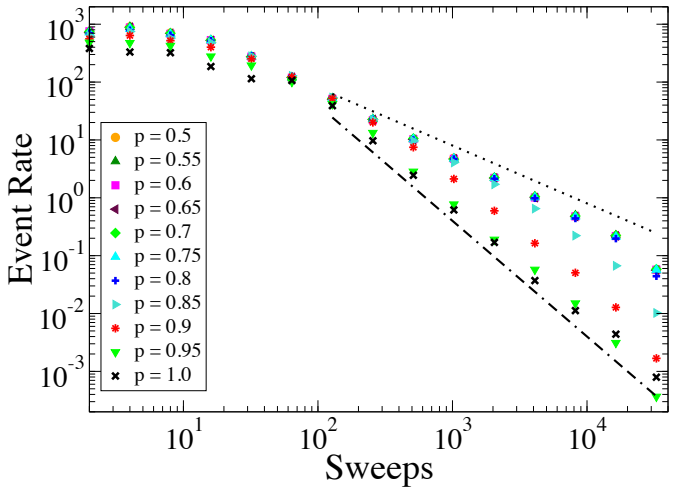

Figure 2.5: Instantaneous rate of record barrier crossing events in EA, as defined in Fig. 2.1, with time after the quench, as described in Fig. 2.2. Asymptotically, for larger times, that rate varies as a power-law with a seemingly hyperbolic decline, $\sim 1/t$ (dotted line), for smaller p to an almost quadratic decline, $\sim 1/t^2$ (dash-dotted line), for larger p.

parently. All the results shown here were obtained for systems with $N = 16^3 = 8096$ spins, using periodic boundaries, since we found very little variation with system size for larger N.

The fact that the underlying ordered state is either glassy or ferromagnetic affords us to also measure the increase in magnetization with time, as demonstrated in Fig. 2.3. This measure actually exhibits a more dramatic transition between the glassy and the ferromagnetic case, as consecutive snapshots of both, of the valley count as well as the magnetization, are shown in Fig. 2.4 for a progression of times that increases by a factor of 8. In these plots, we have also marked the zero-temperature transition at $p_c \approx 0.77$, which proves well consistent asymptotically with the transition out of the glassy relaxation behavior.

Finally, we can also look at the instantaneous rate of barrier crossing events, effectively the derivative of the valley production, i.e, inverting the integral in Eq. (1.4). Indeed, throughout the glassy regime, the rate decelerates roughly hyperbolically, in

accordance with the RD predictions for a logarithmically divergent valley production. [Note that this could miss a minor logarithmic correction, such as $\lambda(t) \sim 1/(t\sqrt{\ln t})$, for instance, needed to get $\sqrt{\ln t}$ for the valley production in Fig. 2.2.] For $p > p_c$, in the ferromagnetic coarsening regime, we notice that the rate falls off increasingly sharper, ultimately about as $\sim 1/t^2$. Consequently, its integral stalls out into the plateaus seen in Fig. 2.2. Apparently, domain mergers occur more rapidly, on a power-law scale, in coarsening ferromagnets. Despite the rapid drop in the event rate, the average domain size manages to increase as a power-law [81], because later mergers expel larger amounts of excess heat. In case of the glass, each event expels on average a fixed amount of heat, roughly. Therefore, both valley production and domain growth proceed similarly (logarithmically), as an integral of the event rate, since each activation has the same impact.

2.4.2 Sherrington-Kirkpatrick Spin Glass

Here, the coarse-graining framework as applied to the Sherrington-Kirkpatrick spin glass and the ferromagnet is shown, with Hamiltonian described in Section 1.1. A family of models are defined, parametrized by α, used in $p = \frac{1}{2} + \frac{\alpha}{\sqrt{n}}$, which is the admixture variable in the bimodal distribution. The reason for this parametrization is that for the SK model, a subextensive excess of ferromagnetic bonds will very quickly result in ferromagnetic behavior, so one cannot assume that having half of the bonds be ferromagnetic will generate glassy behavior. After all, mutual connections between all spins require the number of ferromagnetic bonds to only slightly exceed the number of antiferromagnetic bonds, in order to tip the system into becoming ordered. The transition to the ferromagnetic regime occurs almost immediate beyond a bond density of p = 0.5, with a strong system size dependence, forcing us to adapt a different scale to observe it. To explore a full range of behaviors, α is varied such that $0 \leq \alpha \leq 2$.

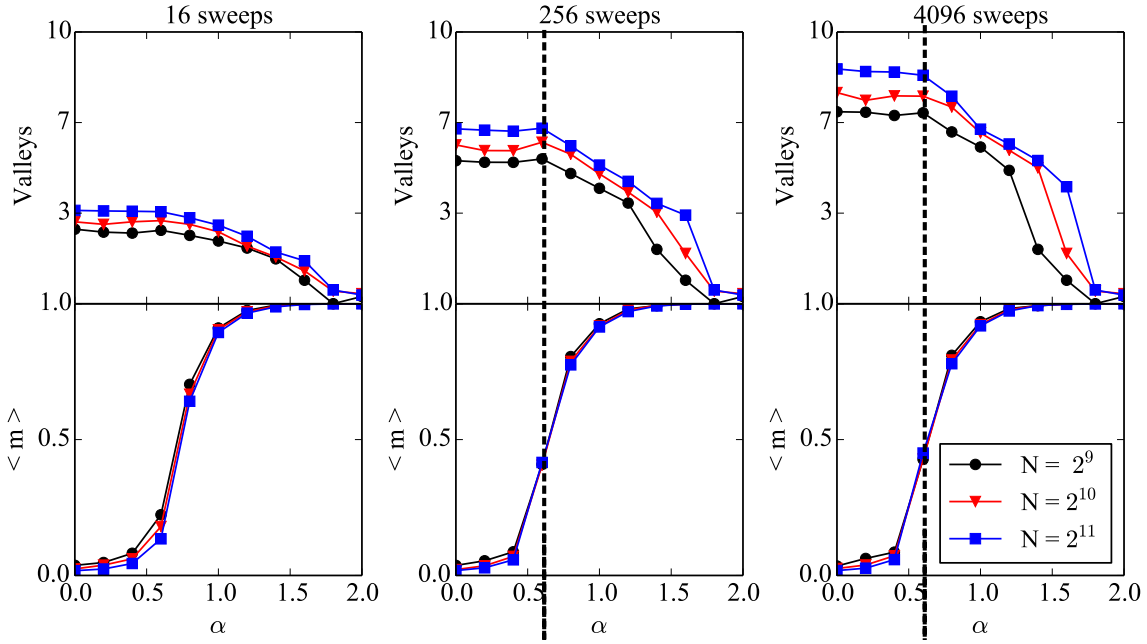

Figure 2.6: Instantaneous average valley counts and magnetization in EA as function of α at different sweep-times $t = 16$, 256 and 4096 from left to right, each for three different system sizes indicated on the legend. The first row shows the average number of valleys, and the second row shows the average magnetization. According to this data, the valley production is time dependent as the sharpness of the transition becomes more pronounced in the later sweeps. In contrast, the magnetization appears to be saturated already early on, predicting the critical threshold within 16 sweeps. Additionally, we see no system size effects when using αas the parameter.

For our simulation, we look at a system size of N = 2048 spins that are quenched from infinitely high temperate $T = \infty$ to $T = 0.7J_0$. We implement the Monte Carlo Metropolis Hastings algorithm (described in the introduction) to generate an ensemble of time traces, which are then coarse-grained according to RD.

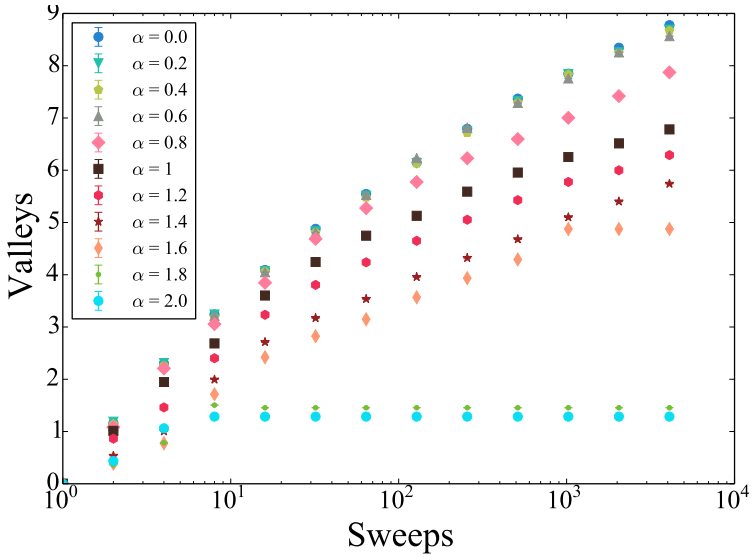

Figure 2.7: Number of valleys traversed during relaxation ensuing after a quench of SK for different bond fractions α from a high temperature $T = \infty$ to $T = 0.7J_0$, averaged over an ensemble of trajectories for $N = 2048$ spins. In the range $0.0 \leq \alpha \leq 0.6$, the number of valleys traversed grows logarithmically and largely independent of α, indicating that the regime is glassy.

Similar to Fig. 2.2 for EA, in Fig. 2.7 we show the numbers of valleys found in a SK system with $N = 1024$ spins. There appears to be a critical threshold at $\alpha_c \approx 0.6$. For $\alpha \leq 0.6$, the valley production increases about as $\log(t)$, essentially uniform with bond density, given the nearly perfect overlap in the data. This is no longer case when $\alpha > 0.6$, where the production of valleys decreases gradually before plateauing completely. While domains in the sense of geometric regions of a certain length do not exist in a mean field system with long-range interactions, individual spins develop clusters of increasingly ordered local fields with some of their neighbors that entrench the system into deeper valleys. It becomes increasingly more difficult for the system

to overcome the energy barrier of flipping the entire cluster, causing the relaxation process to evolve logarithmically, as mentioned in the introduction [81].

That said, evidence of a critical threshold suggests that beyond α_c, the system changes its landscape dramatically. It exhibits an inclination to order rapidly, facilitated by the fact that local fields of individual spins immediately affect all others, as the evolution of magnetization in Fig. 2.9 suggests. Flat interfaces between such clusters, as they may exist between domains in low-dimensional lattices like EA, are absent here and any imbalance in curvature quickly erodes inferior clusters. Therefore, despite the quantitative differences pertaining to local structure between the Edwards-Anderson and Sherrington-Kirkpatrick spin glass, our results suggest that the glassy behavior in both can be attributed to the hierarchical nature of the energy landscape, and the lack of it beyond the transition to ferromagnetic order, seen both in Fig. 2.3 and Fig. 2.9.

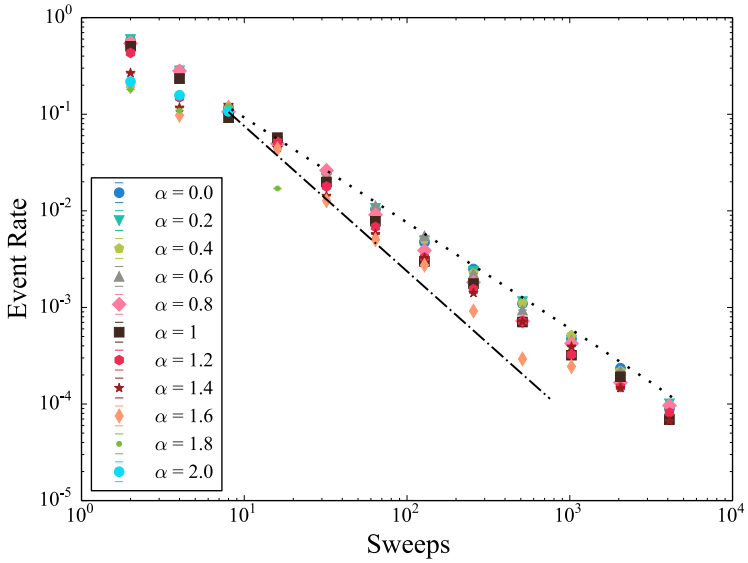

Figure 2.8: Instantaneous rates for the number of record barrier crossings as a function of time, for every α-value in SK. The instantaneous rate decreases as a power-law for all but the highest admixture values. In the glassy regime, the decelerations is essentially hyperbolic (dotted line), while the rate drops more sharply for $\alpha > 0.6$, up to roughly $t^{-1.5}$ at $\alpha = 1.6$ (dash-dotted line), beyond which further record events become immeasurably rare.

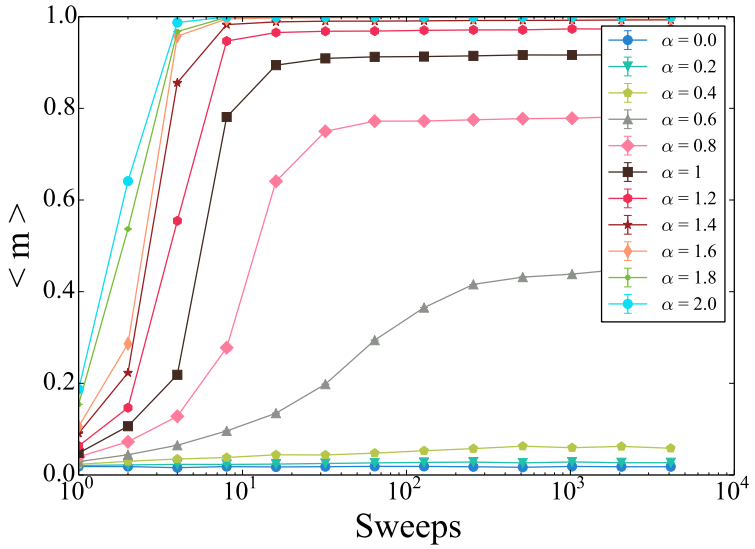

Figure 2.9: Average magnetization for SK in the same simulations shown in Fig. **??**. According to this measurement, the system begins to order at $\alpha_c \approx 0.6$, since a non-zero magnetization in the long-time limit indicates that majority of the spins have ferromagnetically ordered. The transition in magnetization shown here is far more dramatic than in the valley counts, but nevertheless affirms the same critical threshold.

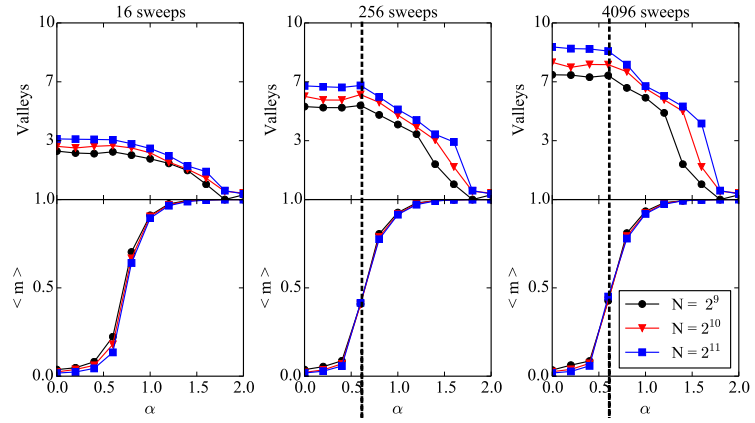

Figure 2.10: Instantaneous average valley counts and magnetization in SK as function of α at different sweep-times $t = 16$, 256 and 4096 from left to right, each for three different system sizes indicated on the legend. The first row shows the average number of valleys, and the second row shows the average magnetization. According to this data, the valley production is time dependent as the sharpness of the transition becomes more pronounced in the later sweeps. In contrast, the magnetization appears to be saturated already early on, predicting the critical threshold within 16 sweeps. Additionally, we see no system size effects when using α as the parameter.

The evolution of valley counts across different system sizes was also studied, only to find a minimal dependence of the transition on larger size, as shown in Fig. 2.10. While the relationship (or lack thereof) between the number of valleys encountered and the bond admixture exhibits time dependence, the critical threshold with regard to ordering already emerges after about two hundred sweeps.There is clearly an agreement between valley statistics and the ferromagnetic order parameter in suggesting $\alpha_c \approx 0.6$ as the critical threshold.

Lastly, the deceleration of the rate of record barrier crossing events in Fig. 2.8 were studied. Clearly, the rate decays with a power of time t. While there is a steeper deceleration in the barrier crossing events for larger α-values, the difference between the exponents is quite subtle on this time scale within our simulations. In the glassy regime, $\alpha < \alpha_c \approx 0.6$, the rate clearly decays hyperbolically, as consistent with RD, whereas it falls off steeper above α_c. However, for values $\alpha > 1.6$, the fall-off becomes so significant that new valleys are not encountered beyond the first ~ 100 sweeps.

2.5 Conclusion

This study explored the distinction between glassy relaxation and ordinary coarsening, which is often ignored in the description and analysis of aging systems. Focusing on families of models that interpolate between either extreme, we not only apply measures [88, 89] that clearly indicate the difference but also show a rather sharp transition in the nonequilibrium behavior between those extremes that, for the Edwards-Anderson model on a cubic lattice, appears to coincide with the (equilibrium) zero-temperature transition between spin glass and ferromagnet [90].The corresponding transition that we find at a subextensive scale in SK seems to have been unnoticed. While the distinction we are making between a coarsening (ferromagnetic) and an aging (glassy) regime can be seen as semantic, considering that

both, algebraic as well as logarithmic growing domains, are commonly portrayed as coarsening [81], the difference in dynamic behavior after a quench is profound. The picture that emerges is one of a largely convex landscape on one side with invariant energetic barriers in the case of coarsening, a system that despite its often complex network of fractal interfaces locally homogenizes rather quickly. On the other side, we find a very hierarchical landscape [91, 92, 93, 94, 28] with energetic (and potentially entropic) barriers that grow with deeper entrenchment within the landscape, rendering all but record fluctuations ineffective for relaxation. From this study, it can also be confirmed that the aging protocol can act as "landscape classifier" that reflects the complexity of a system (i.e whether or not it needs "feedback" to learn more about the global landscape). In the future, this kind of analysis can potentially help understand whether certain landscapes are actually learnable, which can help inform what kind of questions (depending on the structure of their landscape) can and cannot be solved by learning algorithms.

Chapter 3

Hierarchical Landscapes and Memory

3.1 Summary

The content in this chapter is primarily taken from the pre-print, "Real-space model for activated processes in rejuvenation and memory behavior of glassy systems" by Mahajabin Rahman and Stefan Boettcher, available through this link: https://arxiv.org/abs/2209.00794. For full disclosure, this manuscript is still undergoing changes after feedback from two rounds of reviews. As this work re-introduces debates from the early 2000s, we are continuing to reconcile our work with previous literature, which means that we will further refine our framing of the problem and hone our understanding as to where our work stands in the debate regarding the extension of mean field machinery to finite dimensional systems.

In the previous section, we used ferromagnets and two classes of Ising spin models as our two separate landscape structures and use RD to see if the essential features of their dynamics, unique to those structures, can be captured with RD. The affirmation that RD is a viable alternative to using the growing length scales (an averaged value)

as a measure of "ordering" also means that coarse-grained rare events can still capture the most essential dynamics of the system at least as well averaged measurements.

In this chapter, we effectively do the reverse – we use a model specifically designed to record dynamics, to see if we can infer a hierarchical structure by identifying rejuvenation and memory effects (signatures of the hierarchy). Ultimately, our study points out a simple and alternative perspective to the myriad of literature in which mean field theory is central to memory effects. Thus, both models that are mean field based, and activated processes based, may be used to study aging.

3.2 Introduction

Memory introduces non-monotonic effects in the relaxation process of some disordered systems. Effects related to memory can be seen through momentarily perturbing the conditions in which the systems relaxes in. The archetypal example involves a temperature shift. When a spin glass, for example, is quenched from $T > Tg$ to $T_1 < T_g$, the spin glass starts to age, as we already know. However, after a second downward quench from T_1 to T_2, there is a re-initialization of the aging, meaning that the spin glass starts to behave like a younger version of itself, hence called rejuvenation. When the spin glass is reheated back to T_1, it is able to recall its last "state" before the second quench, and evolves from there, proving that it has memory. This non-monotonic behavior is considered to be rather puzzling and for that reason, rejuvenation and memory effects, especially in spin glasses, have been studied in detail [95, 96] especially in the 2000s. In this part of the research, there are two main points that are addressed: First, another test of record dynamics is conducted – If one wants to make the claim that RD distinguishes glassy systems that have hierarchical landscapes, then it is necessary to check whether anomalous aging behaviors can be reconstructed simply with record dynamics as well. If this is

successful, then it fulfills the second purpose of this project, which to explain how aging facilitates memory and rejuvenation with activated processes rather than the mean field description.

Rejuvenation and memory effects have fully been explained by mean field theory, which uses all-to-all connected systems like the Sherrington-Kirkpatrick spin glass. As briefly mentioned in 1.5.1, the physical meaning of analytical results of the SK spin glass points to there being a free energy landscape that is organized hierarchically. That is why downward quenches seem to "re-start" the dynamics, precisely because of the self-similarity as those states. The fact that a complete explanation exists along with analytic tools, makes mean field theory very appealing for other systems that as well. However, analytically, it is unclear whether conclusions from mean field calculations can be applied to finite dimensional systems, such as structural glasses or amorphous systems. Numerical and molecular dynamics simulations have shed light on this, and it appears that much progress has been made recently in characterizing different phases of behavior in particular for structural glasses in the context of mean-field replica theory [16, 7]. Remarkably, some of those predictions – from a physical space with infinite dimensions – are valid all the way down to realistic hard-sphere systems in a two-dimensional plane [26, 42].

This study takes a step back to note that mean field is only one way of understanding aging. A common caveat made in applying those results concern their lack of including collective, activated processes which are expected to supersede some of the microscopic dynamics in the glassy regime. Such activated process set in when significant barriers in the free energy landscape localizes the motion [97, 98], as would be the case for "caging" in a colloidal glass, for example.

Here, we offer an alternative real-space description based purely on activated processes for the understanding of relaxation dynamics in hierarchical landscapes. To this end, we use the cluster model, a coarse-grained lattice model of a jammed system,

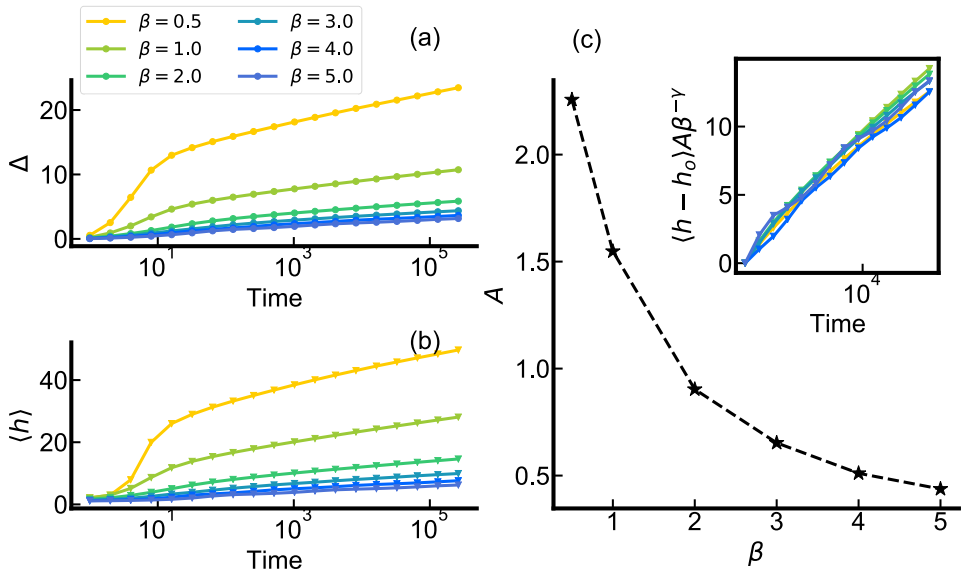

Figure 3.1: Increase of (a) MSD and (b) average cluster size with the logarithm of time, for different values of β in Eq. (3.1). The results show that motion slows systematically with increasing β. Panel (c) shows the dependence of the log-slope A on β in fitting $\Delta \sim A\ln(t)$ to the cluster sizes $\langle h\rangle$ in (b), yielding $A \approx \beta^{-\gamma}$ with $\gamma \approx 0.7$. The inset demonstrates the collapse of the appropriately rescaled data from (b).

which is also a physical incarnation of RD, to analyze rejuvenation and memory effects during aging after a hard quench. In this model, neighboring particles on a lattice aggregate through local interactions into clusters that fragment with a probability based on their size. Despite the simplicity of the cluster model, it has been shown to reproduce salient observables of the aging dynamics in colloidal systems, such as those accounting for particle mobility and displacements. Here, we probe the model using more complex quench protocols and show that it exhibits the same rejuvenation and memory effects attributed to the complex hierarchical structure of a glassy energy landscape [99, 100], and also offers a real space explanation.

3.3 The Cluster Model

The cluster is a simple on-lattice model that is considered a physical incarnation of RD, and has been specifically designed [87] to capture the combined temporal *and* spatial heterogeneity found in a generic aging system, although it particularly resembles jamming in colloids [57]. In this cluster model, particles completely fill a lattice, one on each site at all times. Yet, each particle by itself is either isolated, forming a cluster of size $h = 1$ (known as a 'singleton'), or it is jammed in with adjacent particles as a member of a cluster of size $h > 1$. Isolated particles ($h = 1$) possess independent mobility, those in clusters with $h > 1$ are locked in and require activation to become mobile. At the time of the quench, $t = 0$, all particles are mobile, owing to the prior "liquid" high-T or low-density state of the system. When a site is picked for an update at any $t > 0$, there are two possible outcomes, depending on the state of the particle on that site:

1. ($h = 1$): A mobile particle interacts with a random neighbor and both exchange position, the basic unit of mobility in the model. Whether that neighbor itself was mobile ($h = 1$) or already part of a larger cluster ($h > 1$), the addition of the mobile particles now leads to a (jammed and thus immobile) cluster with $h' = h + 1 > 1$.

2. ($h > 1$): An immobile particle jammed inside a cluster of size $h > 1$ may activate an event with an h-dependent probability per sweep [101],

$$P(h) \propto e^{-\beta h}. \tag{3.1}$$

   If it occurs, such an event will break the cluster and create h newly mobilized particles.

3.3.1 How the cluster model represents RD

Following a quench out of the liquid state of mobile particles, clusters form and break up *irreversibly* to re-mobilize and re-distribute their particles to neighboring clusters. To put this in terms of the record dynamics framework, the breaking of a cluster can be considered a "cage breaking" since particles quite physically become released from the cluster they were a part of. Once there is cage breaking, a large fluctuation that represents the change in free volume (as opposed to change in energy, like the previous section) marks a "record" event. Initially, at the start of the quench, there is a transient period im which clusters break up and accrete quickly, until gradually there is jamming-like behavior – (i.e the average cluster size $\langle h \rangle$ is large enough that it does not collapse in a short time scale). For a sufficiently large value of the external control parameter β (that acts as a density or an inverse temperature), a large fraction of particles soon accrete into jammed clusters that only intermittently break up and almost instantaneously feed their particles into ever fewer, and thus ever larger, neighboring clusters, which in turn necessitate ever larger and thus ever more rare fluctuations, requiring a time *exponential* [81, 29] in the size of those clusters.

The effect of all regular fluctuations that only rarely achieve such a significant event beyond reversible in-cage rattle is coarse-grained into $P(h)$ in Eq. (3.1). Cluster growth ultimately decelerates the dynamics, since only larger and fewer clusters remain, which signifies the slow structural changes that characterizes aging.

Despite its simplicity, the model has already been shown to reproduced [57, 102] salient experimental [53] and simulational [103] results for quenches in colloids. In particular, the two-time mean-square displacement (MSD),

$$\Delta\left(t, t_w\right) = \frac{1}{N} \sum_{i=1}^{N} \left\langle \left| \vec{r}_i\left(t\right) - \vec{r}_i\left(t_w\right) \right|^2 \right\rangle, \tag{3.2}$$

was shown to grow logarithmic as $\Delta\left(t, t_w\right) \sim A \ln\left(t/t_w\right)$, depending on the waiting

time t_w after the quench when the measurement commences. In RD, this is a direct consequence of the $\sim A/t$ decline in the rate of cluster break-up events (such a rate for irreversible events was explicitly verified in experimental data for aging colloids [57]). In Fig. 3.1, we also demonstrate that the proportionality factor A is a function of β, similar to what has been observed for domain growth in spin-glass simulations [104], granular compaction [17], but also for MSD in colloidal experiments at different densities [57].

3.4 The waiting time method

This method orders all possible events in a chronology based on their probability of occurring as shown in Eq. (3.1), thus avoiding rejected moves that occur in conventional Monte Carlo algorithms. Given Eq. (3.1), newly freed particles will join clusters on sub-sweep time scales, meaning that each cluster break-up event will typically moves many particles nearly simultaneously. That said, this method can rapidly telescope into the future within just a few update steps when break-ups become rare, which allows us to explore longer time scales $> 10^{10}$ sweeps. The waiting time algorithm is the following:

(1) First, assign a global time t. Prior to any event, while all the clusters have size (h) of 1, the global time should be set to $t = 0$. This global time is updated every time in the event from the queue occurs.

(2) To create a queue, each of the k clusters is assigned a survival time, $\{\delta\, t_i\}_{i=1}^{k}$, based on its current size h_i according to [105]

$$\delta\, t_i = -\log(X_i)/P(h_i), \tag{3.3}$$

with $P(h_i)$ as given in Eq. (3.1) and made stochastic by employing a random number X_i sampled from a uniform distribution.

(3) Then, the cluster with the lowest $\delta t_{\min} = \min_i \{\delta t_i\}$ is selected to determine the event which takes place, which is either a cluster break-up or an accretion depending on the size of k cluster. After the system reconfigures according to the event selected, the global time is then updated to $t + \delta t_{min}$.

(4) Clusters which have been modified due to the selected event are assigned a new δt. For example, if the event was a breaking of a cluster, then each of the freed particles are each assigned a new δt, which are all expected to be very small, so they are still in the front of queue, which means they will make their moves, before other events. On the other hand, if the most recent update was the growth of a cluster, then the whole cluster gets assigned one δt, which will most likely be larger than the previous δt, placing it closer to the end of the queue.

(5) With the updated queue, repeat step (3).

3.5 Simulation Results

3.5.1 Rejuvenation and Memory

In Fig. 3.2, this simple model is shown to be capable of exhibiting both rejuvenation and memory effects, under the temperature shift protocol. Following Ref. [**Scalliet19**], we employ the MSD given in Eq. (3.2) to define a dynamic susceptibility function

$$\chi\left(t_w, \omega\right) = \beta\Delta\left(t_w + \omega^{-1}, t_w\right), \tag{3.4}$$

where $\tau = \omega^{-1}$ sets a time-window over which the decay of the instantaneous mobility at time t_w is assessed. This function allows us to measure a "rate" of activity, rather than accumulated activity like total mean squared distance (MSD), which would allow easier comparison of the dynamics at different times. Note that in the case of both structural glasses and our model, the parameters to generate the typical

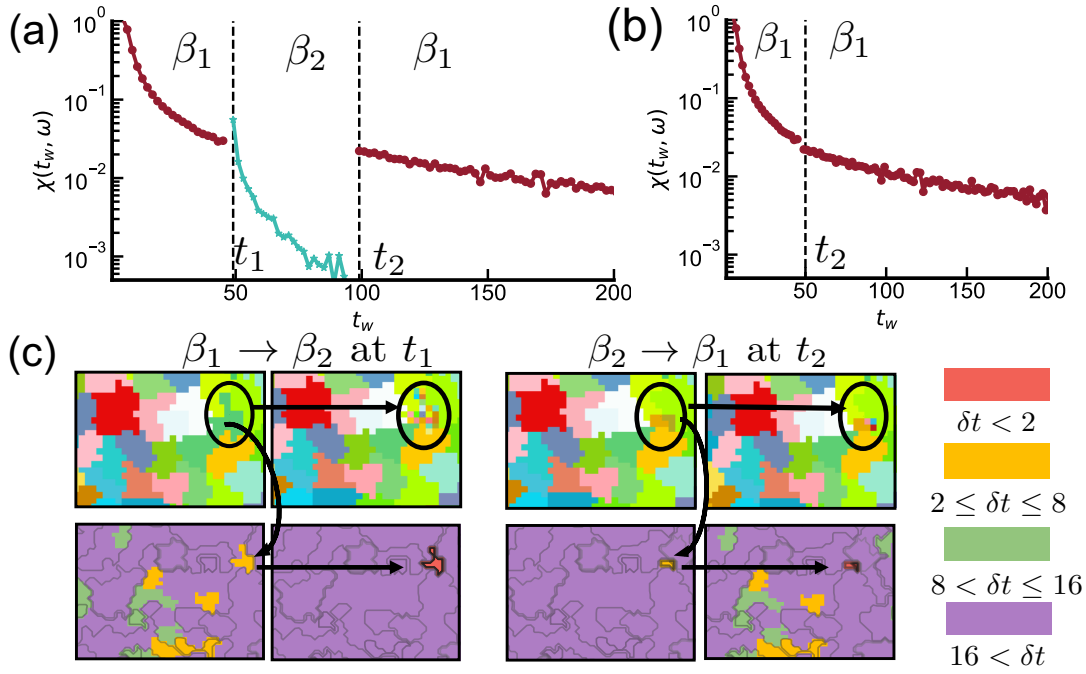

Figure 3.2: Rejuvenation and memory effects produced on an $L = 64$ square lattice subject to a temperature cycle. The system at $t_w = 0$ undergoes a hard quench to $\beta_1 = 0.5$, ages until time (in sweeps) $t_1 = 50$, when temperature is reduced once more to $\beta_2 = 5$. After aging further until $t_2 = 500$, it is reset to β_1. In (a), the susceptibility χ defined in Eq.(3.4) is plotted as a function of t_w using $\tau = \omega^{-1} = 2 \ll t_1$. In turn, (b) shows that χ, when reheated at t_2, is a continuation of the dynamics from the system prior to the second quench at t_1. Both can therefore be "stitched together". In (c), a physical depiction of the situation is provided. The top row shows the cluster formation on the lattice (different colors indicate separate clusters). The bottom row shows the corresponding lattice configuration, here color coded with the survival time δt for that cluster to collapse. The region most affected by the quench at t_1 is circled in all the snapshots. There, some cluster of size $h = 22$ happens to break up and solely its freed particles are able to move during a time window of size $\tau = 2$ after t_1. Right before the lattice is reheated, we see that many of those particles integrated into surrounding clusters, while the remaining ones assembled into a newly formed cluster (yellow), with a longer survival time. Once reheated, the cluster-size distribution is almost identical to the first column, which is why the dynamics seems to pick up where they left off prior to the second quench.

rejuvenation and memory picture (referring to Figure 3.2) require the system to be in a marginally stable state in order to find any dynamics at all deep into the aging regime. In the study that we compare our work to (Scalliet et al., [99]), the marginally stable state was found using a very specific temperature and age of the system, in order to make sure the quench was done right at the cusp of a cage breaking event. The significance of the marginally stable state is discussed in more detail after this chapter in Section 4.2.1.

To produce the statistics in Figure 3.2, the initial quench occurs from an infinite temperature ($\beta = 0$) to $\beta_1 = 0.5$. At that point, χ drops as a function of t_w, using a window size of $\tau = 2$ (in sweeps), while the system is aged up to $t_1 = 50$ sweeps. At that time the system has developed a Poissonian cluster-size distribution with average cluster size reaching about $\langle h \rangle \approx 30$, see Fig. 3.1(b), leaving a number of the smallest and most marginally stable clusters below that size most likely to break. In fact, as illustrated in Fig. 3.2(c), a fraction of those clusters are in the process of steadily collapsing at time t_1 in a large enough system.

At time t_1, a further quench of the system is performed, down to $\beta_2 = 5$. At this much reduced temperature, only clusters below the corresponding average cluster of $\langle h \rangle \approx 3$, as shown in Fig. 3.1(b), would qualify as unstable on this time-scale. Clearly, all of the existing clusters are much too large and are completely frozen at this temperature. Only those currently freed particles from the cluster break-ups that are already in progress can contribute to the instantaneous mobility in this part of the temperature cycle. This small but extensive fraction of mobile particles, in turn, relives the entire history of an aging system freshly quenched to β_2, within the background of otherwise frozen clusters. As in Ref [**Scalliet19**], the overall reduction in mobility Δ is partially compensated by the relative factor of β (here, $\beta_2/\beta_1 = 10$) in the definition of χ in Eq. (3.4). Thus, χ "rejuvenates", immediately jumping up above the previous level reached before t_1, before decaying itself. When the temperature is

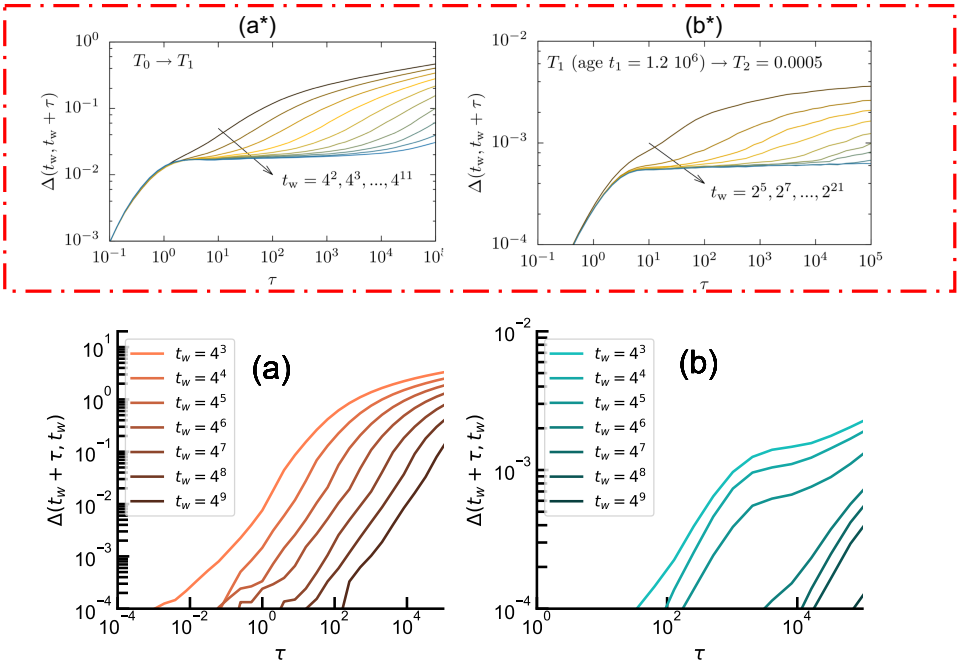

Figure 3.3: MSD in the soft sphere system studied in [99] and MSD the cluster model. The top panel enclosed by the dashed red line shows the results in the original Scalliet et al study. On the bottom panel, (a) after quench to $\beta_1 = 0.5$ (without subsequent temperature changes) and (b) after a subsequent quench at $t_1 = 50$ to $\beta_2 = 5.0$, in the cluster model. In both cases, the quenched system is aged up to certain waiting time t_w, before the dynamics of the particles are measured relative to the configuration at t_w as a function of lag-time $\tau = t - t_w$. Both (a) and (b) show the characteristic dependence of MSD on the age t_w. For (b) this implies that the second quench actually rejuvenated the system, albeit at a much lower mobility due to the lower temperature.

then reset to $\beta_1 = 0.5$ after $t_1 + t_2 = 100$ sweeps, the impact left by the rejuvenating sub-system had a minimal effect on the entire system. Merely those clusters already breaking up at t_1 advanced minutely. Accordingly, its instantaneous mobility returns to the level frozen in at t_1.

3.5.2 Replication of results from soft spheres

Since this study was mostly inspired by a 2019 PRL by Scalliet and Berthier [99], in which the dynamics of soft repulsive spheres were used to look for rejuvenation and memory effects in order to confirm similarities to mean field spin glasses. As

a validation of rejuvenation, Ref.[99] compared the age-dependent (two-time) MSD observed following the initial quench to β_1 with the MSD found after the second quench to β_2 while using its starting point t_1 as the new origin of time.

Indeed, in Figure 3.3 (a* and b*), they demonstrate that in both measurements the two-time MSD behaves analogously, as if t_1 was an entirely independent quench.

To replicate these results in RD, the same setting as in Fig. 3.2 is used in the cluster model, but with a simple quench to $\beta = 0.5$. Now, the system is aged (without second quench) up to various waiting times t_w to measure MSD $\Delta(t_w + \tau, t_w)$ for the lag-time $\tau = t - t_w$. This data is plotted in Fig. 3.3(a), which reproduces Fig. 3 of Ref.[99]. It demonstrates that a system that was aged up to a time t_w remains confined for a corresponding time $\propto t_w$ before exhibiting any discernible MSD. Incidentally, this fact, as well as a collapse of this data as function of t/t_w, was previously explained for experiments on colloids in terms of RD in Ref.[57]. Although mean-field arguments would suggest that MSD after a transient should saturate at long times [106], the existence of activated dynamics in real systems induce further (logarithmic) growth.

More importantly, the rejuvenation effect seen in Fig. 4(a) of Ref. [**Scalliet19**] is captured for the cluster model in Figure 3.3(b) which presents the two-time MSD of particles for several t_w during the second stage of the temperature cycle. Having undergone the initial quench to $\beta = 0.5$, the dynamics are evolved up to time $t_1 = 50$ sweeps, at which time the system is cooled down even further to $\beta = 5$. Once the particles are quenched to the second temperature, they are aged up to a given waiting time t_w, now taking t_1 as the new origin of time. As above, the dynamics are measured as a function of lag-time $\tau = t - t_w$ for each t_w. While the MSD after the second quench differs by a magnitude compared to Fig. 3.3, the t_w dependence shows that rather than continuing the dynamics from the prior quench, the process re-initializes and dynamics are refreshed based on t_w, the age of the system following the second quench at t_1. It is apparent from this analysis that in the cluster model

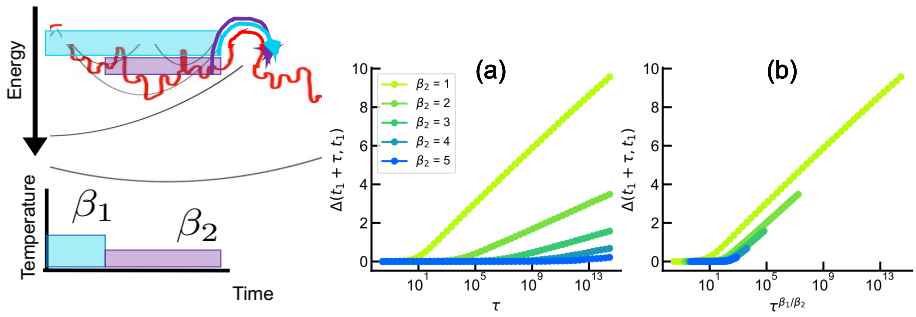

Figure 3.4: Demonstration for the end of of memory. The protocol for demonstrating the end of memory is shown here. In the most left panel, the matching highlighted colors of the β values and highlighted parts of the energy trace, show that the quench determines what parts of the landscape the system can explore. In (a), we measure the MSD $\Delta(t_1+\tau, t_1)$ for particles in the cluster model initially quenched to $\beta_1 = 1.0$, then aged for $t_1 = 25$ sweeps, when it undergoes the second quench to β_2. The system remains entrenched in its metastable state attained at t_1 for a time $\tau = \tau_2$ that depends on β_2, before significant displacement occurs that erases the memory of that state. In (b), this data collapses when τ is rescaled according to Eq. (3.5).

the intervening quench to β_2 (if it is not excessively long, see below) leaves little mark on the large fraction of frozen-in clusters, which on re-heating at t_1+t_2 continue their mobility where it froze in at t_1.

We note that, unlike in Figs. 3 and 4(a) of Ref [99], the coarse-grained motion in our model *by design* eliminates both, the (trivial) initial ballistic motion and the subsequent rattle particles experience at the shortest times while confined within their cages. Thus, the lower plateau visible for the continuum MD simulation there, due to rattle within a finite-sized cage, is strictly zero for particles that are bound to discrete lattice sites until an event occurs.

3.6 Predictive power of the cluster model

Finally, we point out that the cluster model reproduces other properties predicted for systems exhibiting rejuvenation and memory effects. For instance, for spin glasses it was shown in Ref.[97] that the memory effect may diminish for a very long, intervening

rejuvenation stage. In Fig. 3.2, the system ages from the initial quench at temperature β_1 and at t_1 has entrenched itself in a metastable state of some free-energy barrier ΔF. To escape the memory of that state at β_1, a record fluctuation is needed, which according to RD typically occurs at time $\tau_1 \approx t_0 \exp\{\beta_1 \Delta F\}$ with $\tau_1 \sim t_1$, where t_0 is some system-specific microscopic time. Quenching anew at t_1 from β_1 to β_2 leaves the system even deeper entrenched within *that* state, now needing a time $\tau_2 \approx t_0 \exp\{\beta_2 \Delta F\}$ to escape and loose its memory. Thus, reheating at a time $t_2 \gg \tau_2$, i.e., a time beyond

$$\tau_2 \sim B\, t_1^{\beta_2/\beta_1}, \tag{3.5}$$

with some constant $B = t_0^{1-\beta_2/\beta_1}$, memory will have been lost. In Fig. 3.4, we demonstrate this effect in the cluster model.

3.7 Conclusion

The main takeaway from this study is that in addition to mean field tools, activated processes can purely account for rejuvenation and memory. The cluster model, despite being extremely minimal, reproduces the macroscopic observable rejuvenation behavior of the structural glass studied in Ref. [99]. However, some of their conclusions can be qualified. For one, that these results fit well with predictions of mean-field theory should not necessarily be taken as evidence that all aspects of the theory apply to real systems. As our dramatically simplified model suggest, an elementary description of the requisite hierarchical landscape features [57] may exist that the much more intricate mean-field theory also *happens* to provide. It does not follow that all aspects of that theory apply. Rejuvenation and memory by themselves are not even sufficient to imply glassy behavior [96].

In Scalliet paper, it is suggested that all particles partake in the rejuvenation phase, i.e the entire system resets. Clearly, in the cluster model, rejuvenation works

because majority of the system freezes at T_2, whereas a subset of particles are mobile, but slow down with t_w thus leading to MSD decay. At first glance, it may seem that the cluster model does not actually rejuvenate – however, a closer look at the Scalliet study reveals that the MSD shown is in cage rattling, which is course-grained out in the cluster model. While this may appear as "featureless" and therefore homogeneous, it has been shown that the actual *irreversible* events that drive relaxation during aging are highly intermittent and localized [55], and are likely hidden deep within the large-Δr^2 tail of those pdf. This heterogeneity is exactly what is captured by the break-up of clusters in our model, after coarse-graining out the in-cage rattle, as that rattle only rarely amounts to meaningful (record-sized) displacements [107].

Lastly, like in other structural glasses, demonstrating rejuvenation and memory effects does require calculating the marginally stable states, where clusters are on the cusp of breaking. When the temperature is changed exactly at a marginally stable state, a collapsed cluster will then have self-similar events on a smaller length scale and faster time-scale. While not addressed in this study exactly, it is clear that being able to understand and target marginally stable states is pivotal if one wanted to "trigger" record events. In the next section 4, marginal stability is an underlying theme that is studied through driven methods such as hysteresis.

Chapter 4

Creation of critical avalanches

4.1 Summary

The Sherrington-Kirkpatrick model has special properties – its dynamics specifically chooses ground states that are marginally stable (and not just meta-stable). Through hysteretic driving, the marginally stable spins become mutually frustrated with one another, which ends up facilitating criticality. In this work, we introduce modified versions of hysteretic driving to trigger criticality in a sparse system (the cubic Edwards Anderson lattice) using what we know about the mechanism in which mutual frustration arises in SK.

4.2 Introduction

Through studies of relaxation processes in the in non-equilibrium systems in the previous sections of this thesis, it has been reinforced that avalanches drive the complex evolution of a system through successive metastable states, determining the time-scale and length-scale (if in real space) of the system's dynamics. However, it has not yet been emphasized that equally pertinent as avalanches, is the way in which they arise. In the naturally occurring processes discussed, like aging, the avalanches

are brought on by a series random fluctuations within the system with a probability of $P = 1/t$. These large avalanches are possible due to marginal stability, which describes the state of the system when the smallest perturbation can initiate collective behavior. In terms of the cluster model discussed in section 3 or the soft sphere model in [108], it is immediately prior to a cluster collapsing and subsequently launching a period of increased mobility, or soft spheres about to undergo an abrupt cage breaking after a period of localized vibrations, respectively. Various studies in the past have articulated that marginally stable states are non-generic and their basins have special characteristics within the energy landscape: For example, [109] points out that the energy landscapes structural glasses evolve through have varying regimes which can be accessed by tuning temperature and packing structures (densities) of the glasses. Depending on those parameters, the glasses may be in the vicinity of the jamming transition where collective excitations help overcome complex barrier structures, or further from the jamming regime where there are low frequency localized excitations, resembling two-level systems [110, 111] where a system has effectively one barrier which can be sufficiently small for tunneling. In addition to the transitions within the landscape, [109] also demonstrates that whether or not a glass/amorphous system *evolves through* the marginally stable state depends on the nature of the glass itself, such as its density, preparation history and previous states. To some extent, the discussion around marginal stability in SK mirrors this point as well. [112] discusses the widely held notion of the Edwards hypothesis, that the ground state which the SK spin glass converges to is based on entropy maximization, is incorrect – in fact, the SK dynamics specifically chooses a marginally stable state with specific properties that will be discussed quite extensively in this section. Therefore, the characteristics of a local minimum, whether it is a marginal state or not, determines the nature of its avalanche – i.e how large it will be, whether it will have a characteristic length scale, and so on. This is particularly important for driven disorder, where avalanches

can be triggered, but understanding the relationship between the marginally stable state and the driving mechanism can help better tune the distribution of avalanches.

From the two previous projects, it is clear as to why being able to tune to marginally stable states is useful - in fact, in [99], parameters to create rejuvenation and memory effects in the first place are chosen based on [109], from a phase diagram mapping the evolution of glasses from different preparation states to marginal stability. An even simpler point is that if one had the power to skip over the states where there is no activity and skip to the marginally stable state, then this can potentially be used to create adaptive optimization heuristics as well for problems that have intrinsically different landscapes and accompanying barrier structures.

In this section, we zoom in on the marginal stability in the SK spin glass in more detail, in particular the manner in which its interesting properties came into observation as this background directly influences our problem formulation in the later section 4.2.2. Just as the research on aging in section 1.6.1 was first contextualized through the coarsening of interfacial dynamics, the exceptional properties of SK convergence to metastable states can be contextualized through driving interfacial dynamics [64]. The latter is typically interesting due to a phenomena known as the depinning transition – this is when a continuous external force f is driven through media with quenched disorder, but the force has no effect on the interface because it is "pinned" and will only move when the force reaches $f = f_c$, where f_c is a critical threshold proportional to the degree of disorder. As an external force approaches f_c from eiher $f < f_c$, or $f > f_c$, the system undergoes movements in the current interface with specific patterns in its morphology (depinning in the random field Ising magnet (RFIM) creates percolating fractals, for example), that can be described with scaling exponents expressed as $(f - f_c)^\gamma / f$ [113]. This interface behavior was considered to be a generic consequence of moving boundaries in quenched disorder media, until the hysteretic behavior of disordered ferromagnets and spin glasses proved otherwise

[114, 115, 116]. When exposed to a gradually varying external magnetic field, (H, which would act as a force (f) in comparison to the depinning studies), new pinned configurations are generated without any threshold equivalent to f_c. This behavior, termed Barkhausen noise, consists of avalanches of spin flips that follow a power law distribution, and appears *everywhere* along the hysteresis loop [63, 115, 64, 117]. Given the lack of tuning required to achieve this effect, these systems from which Barkhausen noise generates were arguably considered to exhibit self-organized criticality (SOC) [118], described in more detail in the introduction in section 1.6. The validity of calling Barkhausen noise as a manifestation of SOC has been debated, as arguments pointed out that the SOC is a consequence of the infinite range of interactions, rather than self-organization [62, 119, 64]. However, this debate is outside the scope of this work; while it is possible that is a matter of semantics, it does bring up the question of how different driving mechanisms changes the dynamics within the magnet. Thus, more pertinent to our purpose here are studies conducted on random field ferromagnets at various levels of disorder, like in the recent work by Spasojević et al and references therein, in order to understand how different driving mechanisms effect the distribution of avalanches [120]. In this study, we analyze three different driving mechanisms in the SK and EA spin glass, unlike previous studies which focus on random field ferromagnets or sandpile models [120, 121]. We choose the SK and EA spin glass models specifically because "traditional" hysteretic driving has shown that unlike SK, hysteresis on EA does not generate critical avalanches [65]. Rather than having a power law, EA avalanches are sub-extensive, and follow an exponential distribution which can be explained by the fact that interactions are only neighbor to neighbor. Therefore, EA cannot be critical with the traditional hysteretic driving method.

4.2.1 Marginally stable spins and mutual frustration: A Case Study with the SK model

Careful consideration of the most marginally stable spins before the next ramp-up dH in the external field H attributed the critical behavior to the mutually correlated state these spins attain within SK [112, 68]. To first define the terms, stability (h_i) of a given spins_i with the external field H_{ext} is

$$h_i = s_i(\sum_{j}^{N} J_{ij}s_j + H_{ext}) \tag{4.1}$$

as a measurement of the spin's overall frustration with its local environment. To be marginally stable, the minimum stability allowed is 0. It turns out that in certain systems, the distribution of stabilities $P(h)$ have a rather distinct shape, particularly in the $h << 1$ regime, where there happens to be a linearly vanishing density of states towards $h = 0$. Here, a "pseudo-gap" emerges, which is bounded by an exponent θ in the form of

$$P(h) = Ah^{\theta} + N^{\frac{-\theta}{1+\theta}} \tag{4.2}$$

For the SK spin glass, that $\theta = 1$ only for near-zero local fields. We emphasize the characteristics of $P(h)$ in this case, because it does not dynamically emerge based on adopting configurations which maximize entropy, but rather, out of all metastable configurations the SK spin glass can converge to, its dynamics specifically select a marginally stable state, whereas generic metastable states have $P(0)$ not occupied by some small number [112].

Such a marginally stable state allows for the dynamic emergence of mutual frustration. During the relaxation process to a marginally stable state, which is simulated using gradient descent at T=0, the spins with negative stabilities will flip sequentially.

Yan et al [68] gives a rather clear analysis using a random walker as an example: Closer to the "steady state", we know that the weakest spin has a stability that is to the order of $\sim 1/\sqrt{N}$. The change in this spin's stability will then be $\Delta h = 2h$ so $h' = -h\ 1/\sqrt{N}$ so the main point is that the newly stable spin will still be a near zero local field. Once this spin flips, all the spins that are frustrated with its current orientation will drift towards instability by $-2J_{ij}s_is_j \sim -1/\sqrt{N}$, while spins that are satisfied will move by $1/\sqrt{N}$ towards the right of the distribution. Each time there is a spin flip, this keeps repeating — After some time, the weakest spins will be the ones that have drifted from right to left due to increasing frustration with newly flipped spins with stabilities $< 1/\sqrt{N}$. So, a group of mutually frustrated spins emerge dynamically in the linear portion of the $P(h)$ distribution.

This is what sets apart systems that display criticality versus those that do not. Mutual frustration ensures correlated behavior – if one were to impinge on any of the weakly stable spins, then it is likely to launch of series of spin flips. The effect of impinging marginally stable spins on mutual frustration, is what inspires our new driving methods, which are meant to create extensive critical avalanches.

The particular emergence of mutually frustrated marginally stable spins in the SK model is tied to the traditional hysteretic procedure. Broadly, studying Ising spin glasses along a hysteresis loop at zero temperature involves slowly ramping an external magnetic field H_{ext} until a spin becomes destabilized ($\lambda_i < 0$) [63, 122, 67, 123, 68]. The process of relaxing the system following an update of the external field will then involve flipping a causal sequence of destabilized spins, thus creating an avalanche that lasts until all spins are again stable ($\lambda_i > 0$ for all i). This relaxation and destabilization protocol then repeats until magnetic saturation is reached, unless some other termination condition is specified. This protocol is referred to as being 'adiabatic' [120], as it implies a continuous external triggering mechanism that is only applied to initiate an avalanche, but is absent otherwise, which is of course only

realistic in simulations. This protocol also reveals other manners in which properties of marginally stable spins are distinct. The typical ramp dH needed to dislodge the next most-unstable spin in SK is $\sim 1/\sqrt{N}$ while it is $\sim 1/N$ for EA, which is easy to show [68]. Thus, comparing the critical behavior of SK and lack of critical behavior in EA in this driving mode seems inconsistent. In either case, as mentioned in [120], those ramps also appear to be unphysical, considering that in a real experiment one would likely advance the external field via a fixed, constant dH that destabilizes at once a large (sub-)extensive set of spins. This is because advancing the field by an increment small enough to trigger exactly one (or a few) of the spins employed in simulations seems rather difficult in reality [67, 120] and is conducive to deterministic behavior.

4.2.2 Problem Formulation

In a stable configuration, it is $h_i > 0$ for all i in Eq. (4.1), with the most unstable spins being the smallest. These populate the low end, $h \to 0$, of the distribution of all stabilities, say, $P(h) \sim \lambda^\theta$ for some $\theta > -1$. Then, the fraction of spins with stability $h_i < h$ is given by $n(h)/N = \int_0^h dh' P(h') \sim h^{\theta+1}$. Thus, the typical spacing in stability between the weakest spins is given by $dh \sim N^{-\frac{1}{1+\theta}}$ and, accordingly, to dislodge just one (or a finite number) of spins, we need to ramp the field by $dH \sim N^{-\frac{1}{1+\theta}}$ [68]. For SK, it is well-known that $\theta = \frac{1}{2}$ [124, 112, 125], meaning that $dH \sim \frac{1}{\sqrt{N}}$ on average for the adiabatic procedure. For EA it is $\theta = 0$ [125], which makes the difference between consecutive weakest spins, and thus the ramp needed to dislodge a finite number of them in the adiabatic procedure, scale as $dH \sim \frac{1}{N}$ instead. For any realistic driving mechanism applied in an experiment, it stands to reason that dH would be a constant value independent of N [67, 120].

Here, we use two methods in which SK and EA spin glasses can be compared side by side. Two of those methods are N-dependent and are based on what we already

know about the adiabatic protocol. Instead of continuously ramping the external magnetic field until the weakest spin is destabilized, the external magnetic field is changed in fixed increments of $dH = 1/N, dH = 1/\sqrt{N}$ and finally, in $dH = c$, where c is some constant value. This last mode is bound to introduce more stochasticity to the driving method, while the other two will produce deterministic behavior for SK, and only introduce some stochasticity to EA through $dh = 1/\sqrt{N}$. It should be noted that there is very little difference between the adiabatic driving of EA or SK that results in an average $\langle dH \rangle \sim 1/N$ or $\langle dH \rangle \sim 1/\sqrt{N}$, compared to the static driving methods (1) or (2) with constant c, resp. For larger N and small enough c, at most a vanishingly small number of spins $\ll N$ is triggering each avalanche, and the results remain asymptotically unchanged from those found in earlier studies with adiabatic driving [122, 123, 65, 68]. Further, if we drive SK with method (1), almost always no weak spin is in reach of a change dH, resulting in many empty avalanches, since typically $\sim \sqrt{N}$ such updates are needed to dislodge the next weakest spin. Thus, aside from those empty avalanches, driving method (1) for SK will not be different than method (2). Only if we drive EA with method (2), or EA and SK with method (3), could we expect new results different from those earlier studies.

After we compare the effects of each of these three driving modes applied to both models, SK and EA, we find that the N-dependent driving modes have no effect on SK, as the distribution is left unchanged. The N-independent driving mode creates broader distributions for the SK model, which remains critical until dH is large enough to generate super critical avalanches. On the contrary, N-dependent driving modes on the EA generate exponential avalanche distributions within a relatively narrow range. Increasing constant rates create increasingly broader distributions, but the shape of these distributions ultimately have system size dependence as well, and therefore does not achieve critical avalanches. Even though the N-independent method does not produce critical avalanches for EA, we look for possible correlatedness by identifying

a ramping rate that creates a percolation transition.

4.3 Models and summary of methods

We study spin glasses with the Hamiltonian in 1.1 with couplings J_{ij} assigned from a Gaussian distribution with variance $\langle J^2 \rangle = \frac{1}{N}$ for the SK model, and $\langle J^2 \rangle = \frac{1}{2d}$ for the EA model. In the following, we only consider the cubic case ($d = 3$) for EA. The stability h_i of each spin s_i takes into account its coupling with the global external field H_{ext} and with the local field imposed by its neighbors s_j through their mutual bond J_{ij}, as incorporated in equation 4.1.

Using the logic described in section 4.2.1, we use three driving modes to look at the avalanche distribution sizes for both SK and EA models. Unlike the traditional adiabatic protocol, these driving modes do not involve continuously changing the external magnetic field until the weakest spin destabilizes. With the adiabatic method, the average interval (dH) ends up being $1/N$ for EA and $1/\sqrt{N}$ for SK, based on the $h \to 0$ regime of the $P(h)$ distributions. Our driving methods are almost identical to the adiabatic method, except we keep a fixed interval dH at which the magnetic field is changed. All three driving methods are initiated in the same manner. Once a bond matrix corresponding to one of the two models is generated, we assign all spins a positive orientation to start with a fully magnetized system. To ensure that this initial configuration is stable, we calculate the original stability values h without an external field, and select an external field $H > h_{\min}$. After this initialization process, the stability values always incorporate the external magnetic field H. First, the ramp is decreased and thus moves in a negative direction in fixed increments of dH. The ways in which we select dH is what ultimately distinguishes the three modes that we explore here:

(1) In the first mode, $dH = c/N$, where c is fixed to 1.

(2) In the second mode, $dH = c/\sqrt{N}$, and c is fixed to 1 here as well.
(3) In the last mode, $dH = c$ where c is a range of values from c = 0.05 to c = 0.8 (we tried higher values that do not give us more fruitful information and therefore decided not to include them here). We decide to explore a wide range of c values to look for potential transitions through a critical point, in which long-range correlations become possible.

We search for transitions in the models in two ways: through avalanche distributions, and through a percolation transition. We know that for SK the avalanches are already critical, but we search to see at what point the avalanches become supercritical.

4.4 Comparison of Avalanche Distributions

In an all-to-all connected model such as the SK, it is likely that given enough mutual frustration [68], even the weakest spin will launch a cascade of spin flips. However, in sparse systems where the weakest spin may be connected only to its closest neighbors, the system will relax rather quickly due to a lack of long range correlations in frustration. Accordingly, it has been found that SK achieves a SOC state [122], whereas EA exhibits only relatively narrow avalanches [123, 65].

Figure 4.1 shows the distribution $P(n)$ of avalanche durations n for the cubic EA lattice and the SK model. The duration n here refers to the total number of spin flips during an avalanche. For adiabatic driving modes, (1) for EA and (2) for SK, the dependence of the ramping rate dH on N ends up imposing an unequal comparison between the two models. Thus, we force the driving modes to be the same to create a side-by-side comparison. In Fig. 4.1, from top to bottom, panels in each row correspond to modes (1), (2), and (3), while the left column refers to EA and the

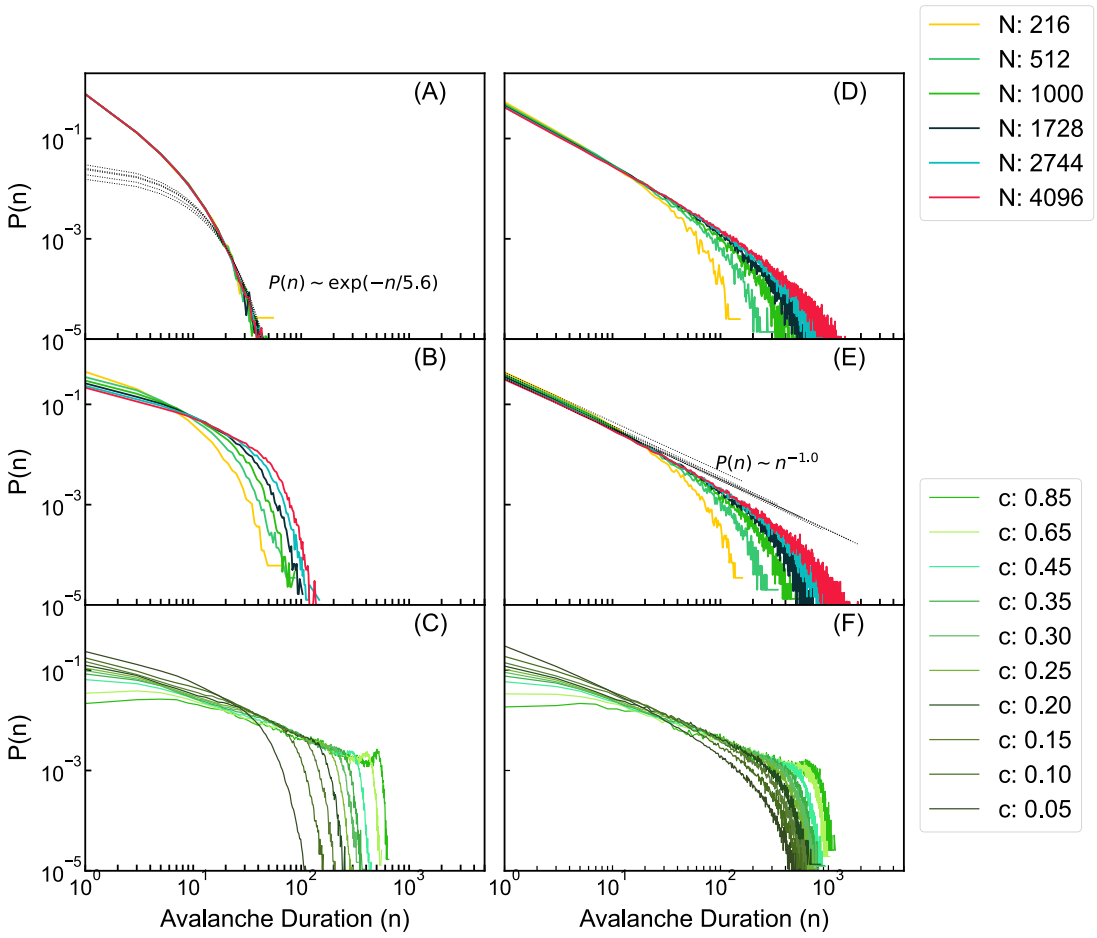

Figure 4.1: The left and right column show distributions $P(n)$ for avalanche durations n (duration is measured by the number of spins that flip) along the hysteresis loop of the EA and SK model, respectively. In each row, (A) and (D) show the resulting $P(n)$ for a ramping rate of $dH = 1/N$ and (B) and (E) for $dH = 1/\sqrt{N}$, for a range of system sizes N. In the bottom row, (C) and (F) show $P(S)$ for $dH = c$ at different strengths c at system size $N = 1000$. Ignoring empty avalanches (D) and (E) for SK are indistinguishable, each showing power-law decay and the size-dependent scaling in the cut-off characteristic of self-organized criticality (SOC), which is absent in (A) and (B) for EA with an exponentially decreasing $P(n)$ where only the sizeable number of uncorrelated spins triggered ($\sim \sqrt{N}$) at each ramp dH affects a perceptable shift. For the size-independent ramp $dH = c$, broader avalanche durations arise in both models with only little sensitivity to c. For the SK model, we see that there is eventually a supercritical transition that leads to a second peak in the distribution at the largest c value. For EA, we notice this peak becomes pronounced much earlier at smaller c values.

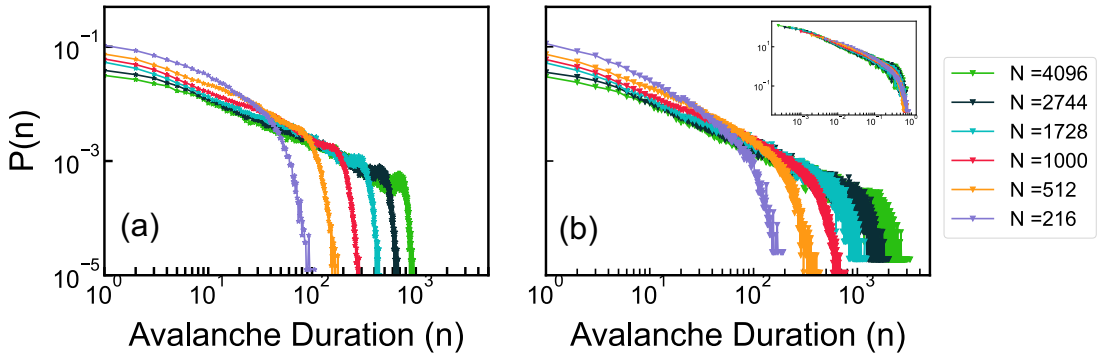

Figure 4.2: The distribution of avalanche durations are shown for different system sizes, with the ramping rate fixed to $dH = .25$. (A) shows the statistics for the EA cubic spin glass, and (B) the SK spin glass with the inset showing the collapsed curves corresponding to (B). For (A), there is a mixture of distribution shapes that demonstrates finite size effects, as $N = 216$ follows an exponential, $N = 1000$ resembles a power law, but for $N > 1000$, the distributions show a peak near $n \approx 10^3$ instead of an exponential cutoff. For (B), every curve follows a power law, $P(n) \sim n^{-\rho}$ with $\rho = .9$ with an exponential cutoff at $n*$ that scales with N^{σ} where $\sigma = 1.0$. The exponents σ and ρ are used to collapse the distributions.

right column to SK. As Ref. [68] noted, the SK displays critical behavior all along the hysteresis loop, which is why there is consistently a power law distribution of the avalanches irrespective of the actual driving. Even when driven in mode (3), a power-law distribution of avalanche duration persists, see panel (F). A fixed $dH = c$ in SK means that every ramp typically dislodges $\sim \sqrt{N}$ spins simultaneously, which according to panel (F) creates only marginally broader avalanches as shown in Figure: 4.2 compared to the modes (1) and (2) when $N = 1000$. We also identify the exponential cutoffs (n*) using a similar method to [122], by finding the crossover point from power law to exponential. Then, we find the dependence of $n*$ on N, which is $n* \sim N^{\sigma}$ where $\sigma = .9$. This relation is accounted for in the more precise finite size scaling form,

$$P(n) = A\, n^{-\rho} d(n/N^{\sigma}) \tag{4.3}$$

where $\rho = 1$, A is an N dependent prefactor, and d is a function of n and the cut off

N^{σ}. Since $N \to \infty$ means that $n* \to \infty$, an infinite system would not have a cut off, affirming self-organized criticality (SOC).

For EA, avalanches along the hysteresis loop closer to saturated magnetized states hardly occur, since there is rarely enough mutual frustration in the system. Naturally, the largest response to a ramp can be expected at the point where the susceptibility, $\chi = dm/dH$, is highest (usually close to coercion, i.e., when $m = 0$ at $H_{\text{ext}}^{\text{coer}}$, see Fig. 4.3 or 1.3). However, in the adiabatic driving, i.e., mode (1) for EA, at no point along the loop achieves avalanche sizes with a correlation length anywhere close to system size, as panel (A) in Fig. 4.1 demonstrates. Yet, to facilitate a "fair" comparison with SK, EA would at least have to be driven in mode (2). With the spacing between the most marginal stabilities h_i being $\sim 1/N$, ramping with $dH \sim 1/\sqrt{N}$ should dislodge $\sim \sqrt{N}$ spins simultaneously throughout the lattice, while SK in this mode merely triggers a finite number of spins. Still, there is no criticality in form of a correlation length cut off by system size, as panel (B) in Fig. 4.1 shows. Merely a shift in the overall duration S of avalanches is observed that is commensurate with the increase in the number of dislodged spins. We can conclude that asymptotically those $\sim \sqrt{N}$ small avalanches triggered simultaneously throughout the lattice each remain too localized to blend into larger correlated domains of flips that could percolate the system. Thus, even for this side-by-side comparison of SK and EA in mode (2), the conclusions of Refs. [123, 65] remain applicable. Only increasing the ramping rate to mode (3), as in panel (C) of Fig. 4.1, can clearly induce sufficiently correlated spin-flip behavior in EA to span the system. It turns out that method (3) does create spanning avalanches in EA, but broad distributions are not necessarily an indication of the correlatedness of the spins. It is expected that when the external field changes in large increments, more spins will flip whether or not their activity is correlated. These distributions alone cannot conclude as to whether there is critical behavior, since a similar collapse to SK is not possible here.

In EA, the distributions are dependent on both N and c. Figure 4.2 (A) shows that smaller system sizes at $dH = 0.25$ remain exponentially distributed. It seems that power law behavior can be seen until larger n where peaks in the distribution arise, rather than an exponential cutoff. These peaks become more pronounced with larger system sizes, and according to Figure 4.1, with larger ramping rates as well, so EA curves clearly cannot be collapsed in the same way as the ones generated through SK.

4.4.1 Limitations on the branching process

A side by side comparison between the Edwards Anderson and mean field model in Figure 4.2 makes salient that "excess" spin flips are allowed to occur but the maximum size of avalanches are still suppressed in EA due to a constraint that has an increasingly stronger effect as system size increases or, as shown in Figure 4.1, as the rate at which the external field is changed. We learn that this constraint is related to the fact that in the Edwards Anderson model, the number of spins that flip during an avalanche is proportional to the number of spins that have have been dislodged in the first place, so in other words, on average, $\langle n/d \rangle = \alpha(c, H)$, where d is the number of spins that have been destablized, or dislodged, in order to initiate an avalanche, and α is fixed for the system size, but is dependent on H, since the avalanche activity changes depending on the location of the hysteresis loop. The relationship between n and d is very similar to the notion of a critical branching process, in which one constituent of a critical system would impact (destabilize, in this case) another constituent, and when this dynamic propagates throughout the system [126], an avalanche is created. Therefore, the critical branching process parameter is the ratio of the number of spins that become perturbed to the number of spins *those* spins then perturb. If $n = d$, then clearly there is neither critical nor correlated behavior, but $n > d$ indicates that there is some level of mutual frustration that is allowing the system to explore more

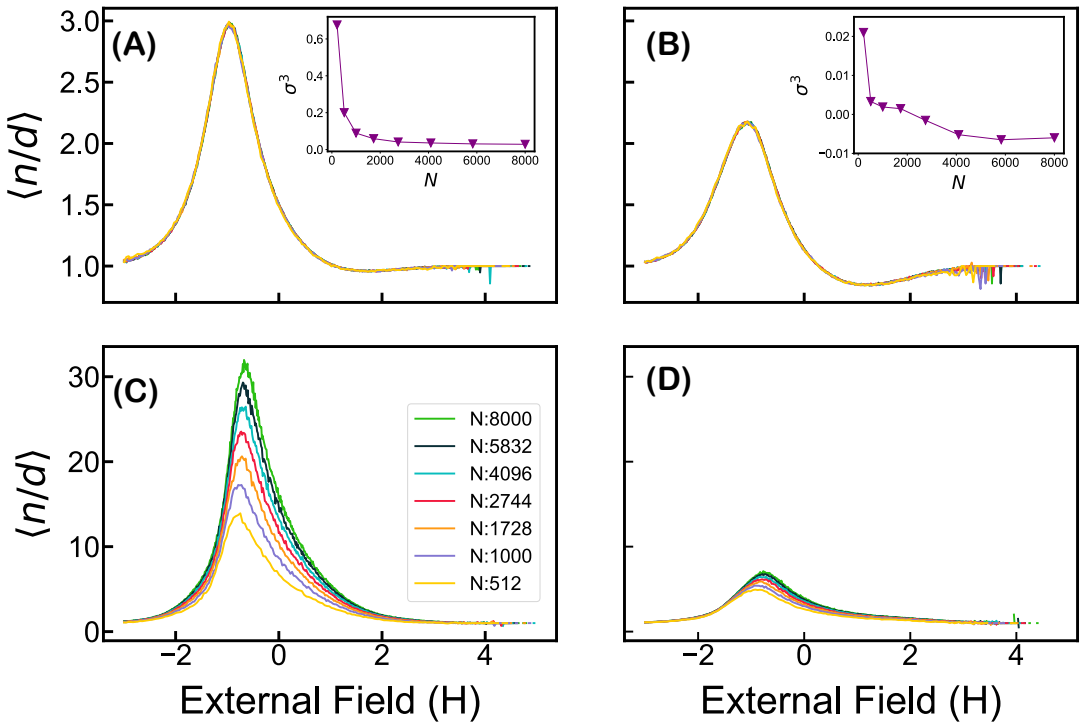

Figure 4.3: Difference in "branching" process in SK and EA at two fixed c values. The "branching" process refers to the number of the spins that flip during an avalanche n as a result of the number of spins dislodged in the first place d. The main panels show $\langle n/d \rangle$ as a function of the external magnetic field (H), since avalanche activity varies along the hysteresis loop. (A) and (B) show the $\langle n/d \rangle$ for EA, whereas (C) and (D) show $\langle n/d \rangle$ for SK. (A) and (C) offer a clear comparison of EA and SK when $c = 0.25$. In the SK spin glass, as N gets larger, so does $\langle n/d \rangle$, which means that asymptotically, a few dislodged spins can trigger infinite avalanches. In the EA spin glass, the averaged statistics indicate that there is an upper bound for the number of avalanches possible that is set by d. We show in the insets that the distribution of n/d is positively skewed for smaller system sizes, but asymptotically approaches to 0. This means that $\langle n/d \rangle$ is a stronger constraint when system sizes are larger, such that n is capped, but because $d \sim n$, there are excess spins that flip and form a bulge towards the upper limit of the avalanche distribution as seen in the previous figure.

configurations. While all system sizes in EA indicate that there is a well defined average $\langle n/d \rangle$, the distributions becomes skewed less positively with an increase in system size, indicating that asymptotically, d determines an upper bound on the maximum avalanche size. At large N values, the average n/d begins to plateau. Since $d \sim N$, there are simply more avalanches that scale as $\sim \mathrm{O}(d)$ but a constraint imposed on their size, thus creating "excess" spin flips towards the tail-end of the avalanche distribution. Because the n/d cut off is dependent on c, an increase in c decreases the system size in which the excess peak develops. Unlike the saturated avalanche sizes in EA, n/d diverges with system size, indicating infinite avalanches asymptotically given a sufficiently small c, as seen in Figure 4.1. Here, when c is as large as x, the avalanche distribution nearly begins to resemble those of the EA model. We learned that at large c values, even n/d in the SK model begins to converge asymptotically just like in EA. This can be explained by the mechanism that if too many spins become dislodged simultaneously, the opportunity to dynamically build a correlation structure that leads to a critical state diminishes. Then, SK effectively acts as like a sparse model where long-range correlations naturally do not exist. This goes to show that in addition to the marginally stable state having certain properties especially in the $P(h)$ distribution, the driving mode also determines whether or not criticality is reached.

4.5 Percolation

4.5.1 Background

The percolation transition marks the point in which a system begins to facilitate long range connectivity, and can be used to detect correlated activity as an alternative to critical distributions. As a brief introduction, percolation is another simple yet seminal model in statistical physics which is often physically likened of the flow of fluid

through porous membrane since the late 1950s, due to Broadbent and Hammersly [**Broadbent1957**]. It is always formally introduced through a lattice with sites that are marked as either occupied or non-occupied, governed by an occupation probability (p). Adjacent sites that are also occupied are said to maintain a "connection" that would facilitate some flow of information between then. Obviously, small p values indicate a sparsely connected system, but when $p = p_c$, the probability of there being a path from one end of the lattice to the opposite (i.e also referred to as a spanning cluster) is 1; the end-to-end connection is why this is made analogous to liquid permeating from top to bottom. It is this transition through p_c that makes percolation one of the simplest models to exhibit a phase transition, since the system has abruptly gone from locally to globally linked, just from a slight tuning in p. Just from this simple example, it may be easy to see why this is a tool to understand a wide breadth of phenomena that are united by their dependence on forming linkages or transport between components. That said, in addition to lattice models, percolation tools are used to understand conductivity in networks with mixtures of resisting and conducting materials [127, 128], the self-assembly, or gelation of polymer chains into cooperative macromolecules [129], and other various types of information flow from phone networks to disease networks [130]. Since spanning clusters are not always meaningful (like for example, if a percolating path emerged at $p_c \approx 1$), extensive studies have been done previously to identify percolation thresholds that indicate randomly connected paths, rather than paths created through meaningful "cross-talk" between systems' components. Therefore, for our null model, we use the random cubic lattice site percolation studied in [131], where the percolation threshold p_c is reported to be ≈ 0.311.

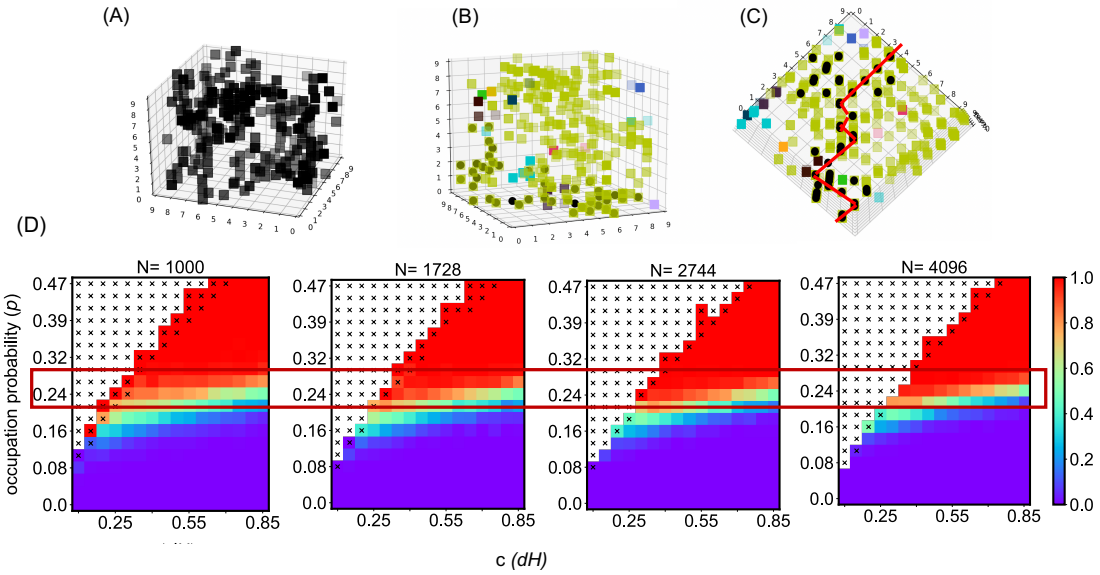

Figure 4.4: The top panel illustratons the algorithm used to identify whether or not a cluster has percolated. At first, all the spins which have flipped are recorded, and are placed into clusters based on a common nucleation site (each color in (B) represents a separate cluster). A path from one boundary to another is identified using a breadth-first search algorithm. On the bottom panel, each grid represents a different system size N, and marks the probability of a percolating cluster as a function of both the constant ramping rate c, and the occupation probability (p), which is equivalent to the fraction of spins which have flipped at least once during an avalanche. Note that each value of c produces a range of occupation probabilities, mostly because the distribution of spin flips changes for EA along the hysteresis loop. Based on these statistics, the threshold at which there is an onset of percolation emerges around $c \approx 0.30$, at a critical occupation probability of ≈ 0.24.

4.5.2 Computational Methods

The ramping rates we use, $dH = c$ does not correspond to a fixed occupation probability. To identify a percolation transition in this model, we identify p_c by using driving mode (3) in the range $.05 \leq c \leq .85$. For every value of c, we examine each avalanche by defining the occupation probability to be $p = n'/N$, where n' is the number of spins which have flipped at least once, which differs from n since a single spin can flip repeatedly during an avalanche. Once p is calculated, we identify clusters of spins that have a common nucleation site. The candidate spanning clusters are then identified by filtering based on whether there are opposing boundary points, and whether cluster sizes exceed $N^{1/3}$. It is easiest to recast the candidate clusters in a tree graph structures, where each spin is treated as a node connected to other nodes, which represent neighboring flipped spins. Child nodes, or descending branches, would represent higher order connections (neighbors of neighbors). Using this structure, the breadth-first search algorithm, which starts at the original node, and visits each branching node until the end, is used to identify whether there are spanning clusters. For each c, we mark whether or not there is a percolating cluster with a 1 or a 0 at encountered values of p, for each trial. Over 5000 trials, we average over P given p, to identify p_c.

In Fig. 4.4, we show that for every value of c there is a range of occupation probabilities that varies only weakly with c. This is consistent with the fact that we see avalanches of different sizes along the hysteresis loop. Clearly, avalanches remain localized for small values c and percolating events occur with finite probability for most of the larger values. When translated into the occupation probability p, we notice that spanning events arise quite close to the well-known threshold of $p_c \approx 0.31160\ldots$ for ordinary site-percolation on a cubic lattice [131]. The indication of a threshold for spanning in this hysteretic avalanching process that is smaller than p_c is a measure of how correlated frustration is among separated spins. As this threshold

of ≈ 0.24 appears to be just below p_c, and to approach it further for larger values of N and c in Fig. 4.4, correlations exist, but they remain rather weak even in this last mode of driving.

4.6 Conclusion

In this paper, the hysteresis protocol was made more stochastic through fixing the ramping rate dH of the external magnetic field at a constant value c to induce long range "correlations" and also be more representative of experimental reality. Driving methods which only target the weakest spin only ever create subextensive activity for sparse systems like the Edwards Anderson model, but having various spins destabilize together creates more frustration, which can potentially lead to more coordinated activity. It is ultimately shown that SK remains critical throughout all modes up to a dh threshold, but EA has exponentially distributed avalanches until the external field is changed as a large enough rate.

To reiterate, a significant and underlying theme in this work is marginal stability. The three different hysteretic driving modes that were central to this paper stemmed from the notion that dislodging a certain fraction of marginally stable spins will change how the correlation builds throughout the hysteretic loop, consequently affecting the size of the avalanches. Indeed, figures 4.1 indicated this to be true since the distribution of the avalanches did show c dependence both for SK and EA. For EA, there is also N-dependence, which is not surprising, since it never becomes critical. To confirm that there is no strong correlation in EA during certain occupation probabilities (which is different from c), we also find that the percolation transition is close enough to the random bond threshold on a cubic lattice. On the other hand, SK is always critical until c becomes so large, that the marginal stable spins no longer retain the mutual frustration they need to, in order to trigger critical avalanches. In

fact, at this point, we see that SK starts to behave much like EA.

One application of this could be in optimization problems. For example, the critical behavior in SK model resulting from hysteretic ramping inspired Ref [67] to liken thermal noise to Barkhausen noise as both create new spin configurations that can help overcome energetic barriers. This resulted in an algorithm alternative to simulated annealing (SA), called hysteretic optimization (HO) which consists of demagnetizing disordered models to arrive at, or towards, their ground state. However, while this hysteretic optimization heuristic (HO) proved successful for SK, it was found to fail to produce the prerequisite critical avalanches in sparse networks of spins, such as for the Edwards-Anderson model (EA), i.e., the Ising spin glass on a lattice. If there is a way to induce long range correlations in a sparse system that do help explore lower energy configurations, then this would provide an avenue to understand information how to learn global landscapes, from local and sparse information. Although the percolation transition indicates that the correlation build up is weak, we do a comparison of hysteretic optimization using different ramp rates in the next chapter.

Chapter 5

Connections to optimization

5.1 Introduction

This section describes work that was inspired by the previous sections along with literature that has been encountered about statistical physics, criticality and combinatorial optimization. It is exploratory in that it connects different ideas to merely brush on how those ideas can be used to modify optimization heuristics. However, surely, there needs to be feedback mechanisms that make the heuristic effective (i.e one needs to understand the "cross-talk" that is happening, and how such coordination between spins (or other parameters) effects the learning of the global landscape from local information). So far, our attempts to understand the feedback mechanisms have been inconclusive. This is a possibility for future direction of study.

5.1.1 Background

The studies of out of equilibrium disordered systems have many parallels to algorithmic processes for optimization in NP hard problems, where the energy landscape, called a "cost" function in this case, require clever local search heuristics to navigate [132, 133]. The parallels are rather clear; past the glass transition for thermal sys-

tems or well into the jamming transition for athermal systems, the energy landscape is evidently hierarchical [40, 7]; its complexity and ruggedness "traps" the glass into metastable states that for long time scales which further slows down the ability of the disordered system to recover to its "ground" state – i.e the state which minimizes the level of frustration. Spin glasses are therefore the archetypal optimization problem, where a number of constraints must be satisfied in order to reduce the overall frustration, and inspiration from this has been salient as simulated annealing, which uses variations in temperature to explore echelons of the landscapes, as a benchmark that newer heuristics are often compared to. However, in developing algorithms for accessing low energy states, the difficulty is often that different heuristics can only access specific kinds of configurations, so they would not work for all class of problems [132]. For example, adiabatic simulated bifurcation has more recently been considered to be a high performance optimization algorithm which recasts the problem into coupled oscillators and relies on bifurcation phenomena to identify the final minimum energy and while it works for the SK and MAX-CUT problems, it fails for sparse systems, similarly to hysteretic optimization (HO) [123, 134, 135]. Additionally, at the heart of both algorithms is to bring the system to a critical state, where small change in a parameter creates large fluctuations in the states the system evolves through, consequently allowing the system to explore a wider range of configurations. While there is a plethora of literature about the effectiveness of algorithms for different kinds of problems, we stick to the criticality-based HO algorithm as a starting point to explore the relationship between critical avalanches, long-range correlations and optimization and base our work on the case-study with the SK model. As mentioned before, our work in the previous section can be useful in this regard because if we know what kind of driving mechanism will facilitate long-range correlations, and maybe more global ordering of the system, then this can potentially help design or modify existing heuristics.

5.2 Problem formulation

As a proof of concept, we look at two different modifications of the HO (hysteretic optimiziation) heuristic, for which the steps will be discussed below in greater detail.

We reiterate the problems with HO: 1) The first reason has already been discussed in the previous section 4.2.1 which is that hysteretic driving is unable to produce critical avalanches in sparse models like the Edwards Anderson spin glass, and cannot find ground states as a result.To address this part, we use our method (3) to modify HO on the Edwards Anderson spin glass, since the percolation transition does indicate weak correlations.

Our solution to (1) is intertwined with our percolation results in 4.4. Clearly, the results indicate weak to no correlations, but what this implies in terms of learning the landscape can be made more clear by modifying the traditional HO algorithm (that is rooted in adiabatic driving) to the version that is based on changing the field in fixed increments of dH. When we test this modified version on the cubic Edwards Anderson spin glass, we notice that barely any improvement, as the average minimum energy reached is around $\approx$ -1.6 when the "true" minimum is $\approx$ -1.8 [136].

We test this modified version on the cubic Edwards-Anderson spin glass of sizes $N = \{10^3, 12^3, 14^3, 16^3\}$, with c values from $dH = [.05, .85]$ in increments of .05

5.3 Methods

5.3.1 HO with constant $dH = c$

We test this modified version on the cubic Edwards-Anderson spin glass of sizes $N = \{10^3, 12^3, 14^3, 16^3\}$, with c values from $dH = [.05, .85]$ in increments of .05. The hysteresis loop starts at $H_n = H_{max}$ where $H_{max} = \max(h_i)$, and use $H_{n+1} = -\gamma H_n$ for every sweep until $H_n < H_{min}$ where H_{min} is the minimum external field needed

in order to flip any spin at all. γ is ultimately what determines the number of loops the algorithm uses to shrink to $H \approx 0$. Because it is possible for smaller c values to perform better simply due to more exposure through the landscape (smaller c indicates more increments along the loop where more configurations can be explored), we decide the number of loops based on the c value in order to make sure the number of steps (η) are conserved. Here, we keep $\eta = 1000$. To ensure this, we calculate γ based on the geometric sequence $\gamma = 1 - \frac{2H_{max}}{\eta c}$ with η in being the total number of steps during the shrinking procedure.

For the actual simulation, for every realization μ, we first start at $\langle m \rangle = 1$ and ensure that all the spins are stable through a gradient descent. Then we ramp the field in increments of c up until H_n, and keep repeating with every newly calculated H_n, until the looping terminates, based on the termination condition given above. Throughout the procedure, the energy value after every avalanche is stored, but once the loop ends, we only retain the minimum energy E^{μ}_{min} seen so far. For every realization, we perform 100 runs, and ultimately calculate $\langle E_{\text{min}^{\mu}} \rangle = E_{\mu}$. This is then repeated for 50 realizations, per c value, and for system sizes, $N = 1000, 1728, 2744, 4096$.

5.4 Results

The results of this algorithm over many bond realizations and a range of c values, is shown in Figure 5.1. A comparison with Figure 4.4 implies that there is a superior balance between preserving the right correlations, and erasing the wrong ones exactly at c values that correspond to the onset of the percolation transition ($c \approx .25$). As expected, the difference is not large as the correlations during the percolation analysis happened to be weak. It is very clear that immediately after the percolation transition, the quality of the local minimum deteriorates, since there spin flips start to become random and retains no information regarding the landscape. Thus, despite

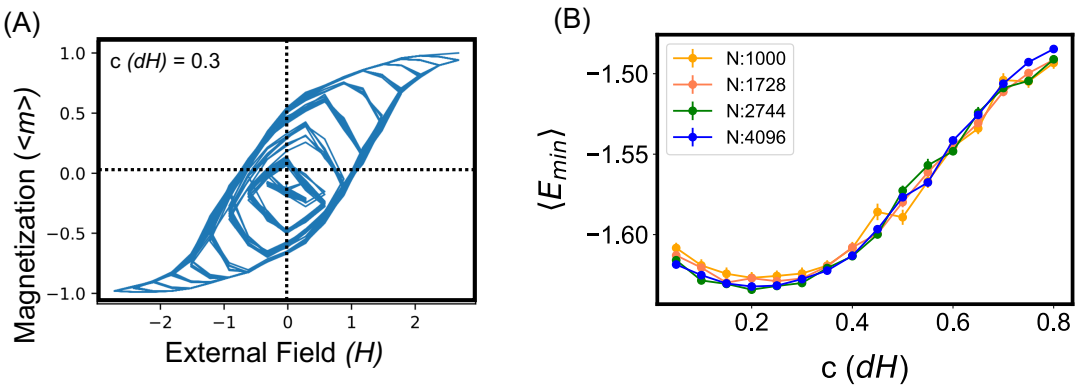

Figure 5.1: Modified HO performed on the EA cubic spin glass. (A) depicts the optimization procedure where the hysteretic loop is iteratively shrunk, and (B) shows the average minimum ground state as a function of c. For each instance (μ), we perform 100 runs for each c value, which returns the lowest energy value seen E^{μ}_{min} at that c. Then, for each c value, we average over all E^{μ}_{min} values over all the runs per instance $< E^{\mu}_{min} >= E_{\mu}$, and then average over all instances $< E_{\mu} >$. There is an alignment between where the lowest $< E_{\mu} >$, and where there is an onset of percolation. At extremely high c values, where percolation is frequent, the system refreshes all the helpful correlation that would have facilitated cooperative behavior. If the c value is too low, the system is more or less myopic and randomly chooses landscape exploration, whereas a balanced c values ensures that the "right" spins are mutually frustrated so that flipping them will encourage the most exploration.

our various ways of trying to create a correlation structure in EA, it seems that hysteretic driving is simply not effective on its own.

5.5 Conclusion and outlook

Hysteretic optimization works by running consequent hysteresis loops but shrinking them progressively, so that external magnetic field is oscillated in smaller amplitudes, as shown in Figure 5.1 The "physical" scenario is then similar to a pinball machine - the magnitude and direction of the external magnetic field directly determines how the landscape is "tilted"; one can imagine that a configuration which is trapped in a local minimum can be aided in its escape by slightly changing the angle of the landscape, allowing the system to "slide out" of a crevice and explore another region. There are, however, two issues here. The first issue is that by adding an external

magnetic field to the Hamiltonian, this process ultimately ends up changing the landscape. While it makes sense to use the Barkhausen noise to "activate" the system into reconfiguring and avoid being trapped in a minima, this method also introduces a bias towards spins of a certain orientation. The second concern is that the protocol requires looping through hysteretic curves [122], without any guarantee that the solution should necessarily improve and is therefore not necessarily computationally efficient. Therefore, our secondary goal is to see if the history can be "redesigned". One way this can potentially be resolved is through an alternative method called EO, where spins are not coupled to the external field. By not creating a field bias, there is no tilt in the landscape, but rather the landscape folds onto itself and by doing so, affects spins of both orientations equally. On top of this, one can potentially use a constant $dH = c$, just like in our previous work, to destabilize spins and correct them , thus "vectorizing" EO (VEO). Our preliminary studies have shown that once again, mutual frustrations play a crucial role — a problem which has been mentioned in the late 90s in a similar parallel procedure [137]. We do find the culprit – Given a large enough c, all mutually frustrated spins will be flipped simultaneously according to VEO rules, but this creates an infinite loop of same group of spins flipping so a stipulation must be introduced such that only a fraction of spins flip, so that the other previous unstable spins become stable in the same orientation they are in – but there are still many questions, as to how one would choose the optimal fraction, and why. Our work on this is still in progress.

Chapter 6

Summary

6.1 Meaning of results

In terms of what was concretely shown, I first address the relationship between aging behavior and landscape morphology. As an alternative to mean field approaches of studying aging, I heavily utilize an approach that is based on purely record events (avalanches or quakes). These are a series of irreversible records that arise from random fluctuations in the aging process, which allow a system to overcome ever higher barrier of metastables states within the energy landscape. These are pivotal because *only* the activation over such barriers allows the system to relax while tumbling into the next meta-basin that is marginally more stable. Within this picture of RD, I show that a clear distinction can be drawn between the coarsening dynamics of an Ising ferromagnet and the aging of the spin glass, which are often put in the same category. I parameterize a class of Ising spin models using the admixture value in order to explore a range of magnetic states from the glassy to ferromagnetic regime. The accumulation of record events grows logarithmically with time in the glassy regime, with a sharp transition at a specific admixture in the ferromagnetic regime where such activations saturate quickly. The implications are rather fundamental, because

the avalanches scaling with barrier height indicates that the dynamics enforce a feedback loop in order to move from metastable states, whereas the invariance of barrier heights points to a different landscape structure, that is smooth.

I also show that the RD picture can be used to understand some of the puzzling behavior of aging disordered systems when they are subjected to temperature shifts, such as rejuvenation and memory. When these effects are realized in mean field glasses, they are attributed to the hierarchical structure of their complex energy landscape, which is seen as a consequence of replica symmetry breaking. The appearance of rejuvenation and memory effects in finite dimensional/structural glasses is then also seen as an indication of replica symmetry breaking, and the use of replica theory is consequently deemed appropriate. Chapter **??** provides a counterexample through the cluster model, which is governed by RD and encapsulates temporal and spatial heterogeneity, but does not have replica symmetry breaking. Numerical simulations of the cluster model show that even with the absence of RSB, the coarse-grained dynamics of the clusters are able to reproduce memory and rejuvenation effects, when put under the same temperature protocol provided that the measurements are taken within a time window where the system falls into a marginally stable state. The model is marginally stable in that clusters are typically large, so majority of the particles are frozen in place except that there is typically one or two small clusters that are on the verge of collapsing. It is only during this time frame where self-similar activities are observed within different time scales. However, this is comparable to previous studies where marginal stability is a necessary condition to measure rejuvenation. Therefore, timescales of the rare events as a reflection of the topology of the hierarchical landscape.

Understanding the relationship between marginally stable states and avalanches led us to earlier work where driven disorder was studied through hysteresis. In many ways, SK can be considered as a "case study" for the dynamics that is capable with

marginal stability physics. Traditional forms of hysteretic driving, considered adiabatic, show that for all-to-all connected models, such as the SK spin glass, hysteretic driving creates a Barkhausen effect, where power law distributed avalanches ensue. This is attributed to the mutual frustration among the marginal stable spins, which create a cascade of spin flips once perturbed. Due to the connectedness of SK, dislodging as few as $\sim 1/\sqrt{N}$ spins will cause the system to be critical. However, such correlations do not emerge in sparse systems. Chapter 4 is based on the premise that perhaps the number of spins which are perturbed account for the lack of avalanche activity in sparse systems. In this chapter, the driving methods I use are inspired by the emergence of mutual frustration among marginally stable spins. Each driving method introduces the same level of stochasticity in both EA and SK, to make an equal comparison between the two. In two of the system size dependent modes, where the ramp rate changes by $1/\sqrt{N}$ and $1/N$, SK avalanches are unchanged as expected where EA avalanches become slightly broader. It is only when the ramping rate changes by a constant that there are significant changes to the avalanche distribution in EA. However, here we discern between critical avalanches and avalanches that occur as a result of more spins being destabilized. While it is suffice to say that EA never becomes critical despite broader avalanches, we are able to detect weak correlation through finding a percolation transition that is slightly below the percolation transition in a random cubic lattice. To understand how these weakly correlated spins manifest, we try to find the ground state of a cubic EA lattice using a wide range of dH into a heuristic that shrinks the HO loop, which has been shown to fail in using traditional hysteretic optimization. While our method does not perform significantly better, there is a clear dip in the average energy almost exactly at a ramping rate where the percolation starts. In order for this to be possible, there must be a feedback loop that is able to create better coordination among frustrated spins.

While we conclude that the number of spins that get dislodged (c) are related to

correlation structure that emerges dynamically, even in the EA model, the mechanism of feedback is rather challenging to study. For starters, why is it that information transmission is optimal at the onset of percolation? While we are able to verify some intuitive hypothesis, the dynamical process has yet to be discovered. One can also look at the intrinsic structure of the bond configurations – what are the characteristics of bond matrices that are more conducive to achieving better minima vs. those that lead to very few coherent feedback mechanisms? Is there fractal structure?

6.2 Broad scientific context

My work has more or less exploited the somewhat polemical nature of glassy and non-equilibrium research; there has always been much controversy in this field – because analytical work is rather limited, there are many debates as to how much the limited analytical conclusions can be extended to different systems. While it is ideal to establish the physics of aging and have it be applied for design materials, there is also the hyperbolic joke that David Weitz once made about there being more theories of glass than the theorists who propose them [138] – we are still unfortunately in a stage where we are learning what kind of parameters "matter", and what the interplay of existing parameters actually looks like and how this translates to coherent length scales. The contribution of this work was mostly to revisit central paradigms in statistical physics and analyze what happens when the assumptions are slightly changed. The first debate here concerns the mean field – if we look at extreme rather than averaged events (which may obscure the rare events), are we able to capture all the main characteristics of the system? Here, we tell the story that gets lost in the field and shed light on the fact that "ordering" is not always a continuous process towards detailed balance, but in fact it is a punctuated process in which a feedback loop is pivotal. The convenience of mean field theory makes it enticing to use for

other systems, so there are ample works that are centered around investigating the validity of mean field to finite dimensional systems, with remarkable results on several occasions. However, while we do not deny that mean field tools are valid for finite dimensional systems, we ask whether such tools need to be necessary if real spaced models based on activated process can reproduce the same dynamics.

Finally, marginal stability seems to play a rather large role in the low temperature physics that is of interest in this work, because these states are conductive to collective excitations given the smallest perturbation. It turns out that only some glasses can have certain kinds of marginally stable states, selected for by their dynamics rather than the Edwards hypothesis – so our work tests if the conditions of one marginal stability state can be artificially created in another state through a parameter that changes disorder and stochasticity. Though a marginally stable state with similar characteristics to that of SK could not extensively be created, it is worth further trying to develop a relationship between the number of perturbed marginally stable spins and structure of feedback loops triggered by the perturbation. While there is no guarantee that this will help optimization, it would help contribute to the general progress in furnishing algorithmic complexity/optimization with soft matter concepts and language.

Bibliography

[1] Rudolf Arnheim. "Entropy and Art". In: *Order A J. Theory Ordered Sets Its Appl.* (2001), pp. 1–50.

[2] P.W Anderson. "More is Different". In: *Science* 177.May (1972), p. 4047.

[3] R. B. Laughlin et al. "The middle way". In: *Proc. Natl. Acad. Sci. U. S. A.* 97.1 (2000), pp. 32–37.

[4] Maya Paczuski, Sergei Maslov, and Per Bak. "Avalanche dynamics in evolution, growth, and depinning models". In: *Phys. Rev. E - Stat. Physics, Plasmas, Fluids, Relat. Interdiscip. Top.* 53.1 (1996), pp. 414–443.

[5] C. A. Angell. "Formation of glasses from liquids and biopolymers". In: *Science (80-.).* 267.5206 (1995), pp. 1924–1935.

[6] M. D. Ediger, C. A. Angell, and Sidney R. Nagel. "Supercooled liquids and glasses". In: *J. Phys. Chem.* 100.31 (1996), pp. 13200–13212.

[7] Patrick Charbonneau et al. "Fractal free energy landscapes in structural glasses". In: *Nat. Commun.* 5 (2014), pp. 1–6.

[8] Kurt Binder and Walter Kob. *Glassy Materials and Disordered Solids - An Introduction to Their Statistical Mechanics*. World Scientific, 2005.

[9] Dapeng Bi et al. "Motility-driven glass and jamming transitions in biological tissues". In: *Phys. Rev. X* 6.2 (2016), pp. 1–13.

[10] Leo P Kadanoff. “From Simulation Model to Public Policy”. In: *Am. Sci.* 60.1 (1972), pp. 74–79.

[11] Alan P Kirman. “Whom or What Does the Representative Individual Represent?” In: *J. Econ. Perspect.* 6.2 (1992), pp. 117–136.

[12] R. K. Pathria and Paul D. Beale. *Statistical Mechanics, Third Edition*. 2007, p. 744. ISBN: 0123821886. URL: http://www.amazon.com/Statistical-Mechanics-Third-Edition-Pathria/dp/0123821886.

[13] Stephen Ornes. “How nonequilibrium thermodynamics speaks to themystery of life”. In: *Proc. Natl. Acad. Sci. U. S. A.* 114.3 (2017), pp. 423–424.

[14] L Struik. *Physical Aging in amorphous polymers and other materials*. Materials Science, 1978.

[15] Ian M. Hodge. “Physical aging in polymer glasses”. In: *Science.* 267.5206 (1995), pp. 1945–1947.

[16] Patrick Charbonneau et al. “Glass and Jamming Transitions: From Exact Results to Finite-Dimensional Descriptions”. In: *Annu. Rev. Condens. Matter Phys.* 8 (2017), pp. 265–288.

[17] Paula A. Gago and Stefan Boettcher. “Universal features of annealing and aging in compaction of granular piles”. In: *Proc. Natl. Acad. Sci. U. S. A.* 117.52 (2020), pp. 33072–33076.

[18] Stuart A. Kauffman and Edward D. Weinberger. “The NK Model of Rugged Fitness Landscapes and Its Application to Maturation of the Immune Response”. In: *Mol. Evol. Rugged Landscapes Proteins, RNA Immune Syst. Proc. Work. Appl. Mol. Evol. Matur. Immune Response, Held March, 1989 St. Fe, New Mex.* (2018), pp. 135–175.

[19] Hans Frauenfelder, Stephen G Sligar, and Peter G Wolynes. "The Energy Landscapes and Motions of Proteins". In: *Science (80-.).* 254.9 (1991), pp. 1598–1602.

[20] John M. Hutchinson. "Physical aging of polymers". In: *Prog. Polym. Sci.* 20.4 (1995), pp. 703–760.

[21] Aniqa Imtiaz et al. "Challenges, Opportunities and Future Directions of Membrane Technology for Natural Gas Purification: A Critical Review". In: *Membranes (Basel).* 12.7 (2022), pp. 1–46.

[22] James P. Sethna. "Order parameters, broken symmetry, and topology". In: *Stat. Mech. Entropy, Order Parameters, Complex.* (2021), pp. 253–286.

[23] Giulio Biroli. "A crash course on ageing". In: *J. Stat. Mech. Theory Exp.* 5 (2005), pp. 291–309.

[24] David Sherrington and Scott Kirkpatrick. "Solvable model of a spin-glass". In: *Phys. Rev. Lett.* 35.26 (1975), pp. 1792–1796.

[25] S.F Edwards and Philip W. Anderson. "Theory of spin glasses". In: *J. Phys. Condens. Matter* 5 (1974), pp. 965–974.

[26] Qinyi Liao and Ludovic Berthier. "Hierarchical Landscape of Hard Disk Glasses". In: *Phys. Rev. X* 9.1 (2019), p. 11049. URL: https://doi.org/10.1103/PhysRevX.9.011049.

[27] Jean Christophe Ono-Dit-Biot et al. "Rearrangement of two dimensional aggregates of droplets under compression: Signatures of the energy landscape from crystal to glass". In: *Phys. Rev. Res.* 2.2 (2020), p. 23070. URL: https://doi.org/10.1103/PhysRevResearch.2.023070.

[28] Paolo Sibani and Karl Heinz Hoffmann. "Hierarchical Models for Aging and Relaxation of Spin Glasses". In: 63.26 (1989), pp. 2853–2856.

[29] Stefan Boettcher and Mahajabin Rahman. "Analysis of landscape hierarchy during coarsening and aging in Ising spin glasses". In: *Phys. Rev. B* 103.2 (2021), pp. 1–8.

[30] C.B. Roth. *Polymer Glasses*. CRC Press, 2016. ISBN: 9781315305141. URL: https://books.google.com/books?id=SQsNDgAAQBAJ.

[31] Martin Goldstein. "Viscous liquids and the glass transition: A potential energy barrier picture". In: *J. Chem. Phys.* 51.9 (1969), pp. 3728–3739.

[32] David J. Wales. "Exploring Energy Landscapes". In: *Annu. Rev. Phys. Chem.* 69.1 (2018), pp. 401–425.

[33] Jin Wang et al. "Quantifying the Waddington landscape and biological paths for development and differentiation". In: *Proc. Natl. Acad. Sci. U. S. A.* 108.20 (2011), pp. 8257–8262.

[34] James E. Ferrell. "Bistability, bifurcations, and Waddington's epigenetic landscape". In: *Curr. Biol.* 22.11 (2012), R458–R466. URL: http://dx.doi.org/10.1016/j.cub.2012.03.045.

[35] Alexander E. Lobkovsky, Yuri I. Wolf, and Eugene V. Koonin. "Predictability of evolutionary trajectories in fitness landscapes". In: *PLoS Comput. Biol.* 7.12 (2011).

[36] Keith D. Ball et al. "From topographies to dynamics on multidimensional potential energy surfaces of atomic clusters". In: *Science* 271.5251 (1996), pp. 963–966.

[37] David Sherrington. "Landscape paradigms in physics and biology: Introduction and overview". In: *Phys. D Nonlinear Phenom.* 107.2-4 (1997), pp. 117–121. arXiv: 9608088 [cond-mat].

[38] G. Parisi. "Infinite number of order parameters for spin-glasses". In: *Phys. Rev. Lett.* 43.23 (1979), pp. 1754–1756.

[39] Giorgio Parisi. "Order parameters in spin glasses". In: *Phys. Rev. Lett.* 50.24 (1983), pp. 1946–1948.

[40] Giorgio Parisi. "The physical Meaning of Replica Symmetry Breaking". In: (2002), pp. 1–15. URL: http://arxiv.org/abs/cond-mat/0205387.

[41] R. C. Dennis and E. I. Corwin. "Jamming Energy Landscape is Hierarchical and Ultrametric". In: *Phys. Rev. Lett.* 124.7 (2020), p. 78002. URL: https://doi.org/10.1103/PhysRevLett.124.078002.

[42] Ludovic Berthier et al. "Gardner physics in amorphous solids and beyond". In: *J. Chem. Phys.* 151.1 (2019). URL: http://dx.doi.org/10.1063/1.5097175.

[43] Stephen Jay Gould and Niles Eldredge. "Punctuated equilibria: The tempo and mode of evolution reconsidered". In: *Paleobiology* 2.2 (1977), pp. 115–151.

[44] David M. Raup. "Biological Extinction in Earth History". In: *Science (80-.).* 231.3 (1933), pp. 1528–1533.

[45] P. Bak and C. Tang. "Earthquakes as a self-organized critical phenomenon". In: *J. Geophys. Res.* 94.B11 (1989), pp. 635–637.

[46] Zeev Olami, Hans Jacob S. Feder, and Kim Christensen. "Self-organized criticality in a continuous, nonconservative cellular automaton modeling earthquakes". In: *Phys. Rev. Lett.* 68.8 (1992), pp. 1244–1247.

[47] M Carlson. "Properties of Earthquakes Generatedd by Fault Dynamics". In: *Nature* 207.5003 (1965), p. 1238.

[48] G. Parisi and L. Pietronero. "Theory of the depinning transition in charge density waves." In: *Epl* 16.4 (1991), pp. 321–326.

[49] Stuart Field et al. "Superconducting vortex avalanches". In: *Phys. Rev. Lett.* 74.7 (1995), pp. 1206–1209.

[50] Adrian Daerr and Stéphane Douady. “Two types of avalanche behaviour in granular media”. In: *Nature* 399.6733 (1999), pp. 241–243.

[51] J. Matias Palva et al. “Neuronal long-range temporal correlations and avalanche dynamics are correlated with behavioral scaling laws”. In: *Proc. Natl. Acad. Sci. U. S. A.* 110.9 (2013), pp. 3585–3590.

[52] Hugo Bissig et al. “Intermittent dynamics and hyper-aging in dense colloidal gels”. In: *PhysChemComm* 6.5 (2003), pp. 21–23.

[53] Peter Yunker et al. “Irreversible rearrangements, correlated domains, and local structure in aging glasses”. In: *Phys. Rev. Lett.* 103.11 (2009).

[54] P. Sibani and J. Dall. “Log-Poisson statistics and full aging in glassy systems”. In: *Europhys. Lett.* 64.1 (2003), pp. 8–14.

[55] P. Sibani and H. Jeldtoft Jensen. “Intermittency, aging and extremal fluctuations”. In: *Europhys. Lett.* 69.4 (2005), pp. 563–569.

[56] A. Fischer, K. H. Hoffmann, and P. Sibani. “Intermittent relaxation in hierarchical energy landscapes”. In: *Phys. Rev. E - Stat. Nonlinear, Soft Matter Phys.* 77.4 (2008), pp. 1–6.

[57] Dominic M. Robe et al. “Record dynamics: Direct experimental evidence from jammed colloids”. In: *EPL* (2016).

[58] Stefan Boettcher, Dominic M. Robe, and Paolo Sibani. “Aging is a log-Poisson process, not a renewal process”. In: *Phys. Rev. E* (2018).

[59] Paolo Sibani, Stefan Boettcher, and Henrik Jeldtoft Jensen. “Record dynamics of evolving metastable systems: theory and applications”. In: *Eur. Phys. J. B* 94.1 (2021), pp. 1–23. URL: `https://doi.org/10.1140/epjb/s10051-020-00039-x`.

[60] Cécile Monthus and Jean Philippe Bouchaud. "Models of traps and glass phenomenology". In: *J. Phys. A. Math. Gen.* 29.14 (1996), pp. 3847–3869.

[61] Cristina M. Marchetti and Karin A. Dahmen. "Hysteresis in driven disordered systems: From plastic depinning to magnets". In: *Phys. Rev. B - Condens. Matter Mater. Phys.* 66.21 (2002), pp. 1–6.

[62] Bruno Alessandro et al. "Domain-wall dynamics and Barkhausen effect in metallic ferromagnetic materials. I. Theory". In: *J. Appl. Phys.* 68.6 (1990), pp. 2901–2907.

[63] G. Bertotti and M. Pasquale. "Hysteresis phenomena and Barkhausen-like instabilities in the Sherrington-Kirkpatrick spin-glass model". In: *J. Appl. Phys.* 67.9 (1990), pp. 5255–5257.

[64] J. S. Urbach, R. C. Madison, and J. T. Markert. "Interface depinning, self-organized criticality, and the Barkhausen effect". In: *Phys. Rev. Lett.* 75.2 (1995), pp. 276–279.

[65] Juan Carlos Andresen et al. *Self-organized criticality in glassy spin systems requires a diverging number of neighbors*. 2013.

[66] Ludovic Berthier and Jean Philippe Bouchaud. "Geometrical aspects of aging and rejuvenation in the ising spin glass: A numerical study". In: *Phys. Rev. B - Condens. Matter Mater. Phys.* 66.5 (2002), pp. 1–16.

[67] G. Zaránd et al. "Using hysteresis for optimization". In: *Phys. Rev. Lett.* 89.15 (2002), pp. 150201/1–150201/4.

[68] Le Yan et al. "Dynamics and Correlations among Soft Excitations in Marginally Stable Glasses". In: *Phys. Rev. Lett.* 114.24 (2015), pp. 1–5.

[69] Miguel A. Muñoz. "Colloquium: Criticality and dynamical scaling in living systems". In: *Rev. Mod. Phys.* 90.3 (2018), p. 31001. URL: https://doi.org/10.1103/RevModPhys.90.031001.

[70] Chris G. Langton. “Computation at the edge of chaos: Phase transitions and emergent computation”. In: *Phys. D Nonlinear Phenom.* 42.1-3 (1990), pp. 12–37.

[71] Mathis Plapp and Jean Frąncois Gouyet. “Dendritic growth in a mean-field lattice gas model”. In: *Phys. Rev. E - Stat. Physics, Plasmas, Fluids, Relat. Interdiscip. Top.* 55.1 (1996), pp. 45–57.

[72] Lucilla De Arcangelis and Hans J. Herrmann. “Learning as a phenomenon occurring in a critical state”. In: *Proc. Natl. Acad. Sci. U. S. A.* 107.9 (2010), pp. 3977–3981.

[73] Giorgio Parisi. “An increasing correlation length in off-equilibrium glasses”. In: *J. Phys. Chem. B* 103.20 (1999), pp. 4128–4131.

[74] P. Mayer et al. “Heterogeneous dynamics of coarsening systems”. In: *Phys. Rev. Lett.* 93.11 (2004), pp. 1–4.

[75] Markus Manssen and Alexander K. Hartmann. “Aging at the spin-glass/ferromagnet transition: Monte Carlo simulations using graphics processing units”. In: *Phys. Rev. B - Condens. Matter Mater. Phys.* 91.17 (2015).

[76] A. J. Bray. “Theory of phase-ordering kinetics”. In: *Adv. Phys.* 43.3 (1994), pp. 357–459.

[77] Z. W Lai, Gene F. Mazenko, and Oriol T. Valls. “Classes for growth kinetics problems at low temperatures”. In: *Phys. Rev. B* 37.16 (1988), pp. 9481–9494.

[78] Marshall Luban and James H. Luscombe. “Equilibrium time correlation functions and the dynamics of fluctuations”. In: *Am. J. Phys.* 67.12 (1999), pp. 1161–1169.

[79] Tatsuo Komori, Hajime Yoshino, and Hajime Takayama. “Numerical Study on Aging Dynamics in the 3D Ising Spin-Glass Model. I. Energy Relaxation and Domain Coarsening”. In: *J. Phys. Soc. Japan* 68.10 (1999), pp. 3387–3393.

[80] Mookyung Chen et al. “Double Transitions and Temperature-Independent Coarsening Dynamics of the Coupled XY-Ising Model”. In: *J. Korean Phys. Soc.* 53.2 (2008), pp. 527–532.

[81] Joel D Shore and James P Sethna. “Logarithmically slow domain growth in nonrandomly frustrated systems: Ising models with competing interactions”. In: 46.18 (1992).

[82] P.G de Gennes. “Dynamics of fluctuations and spinodal decomposition in polymer blends”. In: *J. Chem. Phys.* 72.9 (1980), pp. 4755–4763.

[83] Frank S. Bates and Pierre Wiltzius. “Spinodal decomposition of a symmetric critical mixture of deuterated and protonated polymer”. In: *J. Chem. Phys.* 91.5 (1989), pp. 3258–3274.

[84] Richard A.L. Jones et al. “Surface-Directed Spinodal Decomposition”. In: *Phys. Rev. Lett.* 66.10 (1991), pp. 1326–1329.

[85] W. M.B. Duval et al. “Coarsening in solid-liquid mixtures: Overview of experiments on shuttle and ISS”. In: *Mater. Sci. Technol. Conf. Exhib. 2013, MS T 2013* 4 (2014), pp. 2745–2752.

[86] Wim van Saarlos and Martin Grant. “Domain-growth kinetics of systems with soft walls”. In: *Phys. Rev. B* 37.4 (1988), pp. 2274–2277.

[87] Nikolaj Becker et al. “Mesoscopic model of temporal and spatial heterogeneity in aging colloids”. In: *J. Phys. Condens. Matter* 26.50 (2014).

[88] J. Dall and P. Sibani. “Exploring valleys of aging systems: The spin glass case”. In: *Eur. Phys. J. B* 36.2 (2003), pp. 233–243.

[89] S. Boettcher and P. Sibani. “Comparing extremal and thermal explorations of energy landscapes”. In: *Eur. Phys. J. B* 44.3 (2005), pp. 317–326.

[90] Alexander K. Hartmann. “Ground-state behavior of the three-dimensional +/- J random-bond ising model”. In: *Phys. Rev. B - Condens. Matter Mater. Phys.* 59.5 (1999), pp. 3617–3623.

[91] R G Palmer et al. “Models of Hierarchically Constrained Dynamics for Glassy Relaxation”. In: *Phys. Rev. Lett.* 53.10 (1984), pp. 958–961.

[92] S. Teitel and Eytan Domany. “Dynamical phase transitions in hierarchical structures”. In: *Phys. Rev. Lett.* 55.20 (1985), pp. 2176–2179.

[93] Paolo Sibani. “Random walks on Cayley trees as models for relaxation in a hierarchical system”. In: *Phys. Rev. B* 34.5 (1986), pp. 3555–3559.

[94] Karl Heinz Hoffmann and Paolo Sibani. “Diffusion in hierarchies”. In: *Phys. Rev. A* 38.8 (1988), pp. 4261–4270.

[95] V. Dupuis et al. “Aging, rejuvenation, and memory effects in Ising and Heisenberg spin glasses”. In: *Phys. Rev. B - Condens. Matter Mater. Phys.* 64.17 (2001), pp. 1–7.

[96] Florent Krzakala and Federico Ricci-Tersenghi. “Aging, memory and rejuvenation: Some lessons from simple models”. In: *J. Phys. Conf. Ser.* 40.1 (2006), pp. 42–49.

[97] Jean Philippe Bouchaud et al. “Separation of time and length scales in spin glasses: Temperature as a microscope”. In: *Phys. Rev. B - Condens. Matter Mater. Phys.* 65.2 (2002), pp. 244391–2443911.

[98] Kang Chen, Erica J. Saltzman, and Kenneth S. Schweizer. “Molecular theories of segmental dynamics and mechanical response in deeply supercooled polymer melts and glasses”. In: *Annu. Rev. Condens. Matter Phys.* 1 (2010), pp. 277–300.

[99] Camille Scalliet and Ludovic Berthier. "Rejuvenation and Memory Effects in a Structural Glass". In: *Phys. Rev. Lett.* 122.25 (2019), p. 255502. URL: https://doi.org/10.1103/PhysRevLett.122.255502.

[100] Andrew P. Hammond and Eric I. Corwin. "Experimental observation of the marginal glass phase in a colloidal glass". In: *Proc. Natl. Acad. Sci. U. S. A.* 117.11 (2020), pp. 5714–5718.

[101] Stefan Boettcher and Paolo Sibani. "Ageing in dense colloids as diffusion in the logarithm of time". In: *J. Phys. Condens. Matter* 23.6 (2011).

[102] Dominic Robe and Stefan Boettcher. "Two-time correlations for probing the aging dynamics of glassy colloids". In: *Soft Matter* 14.46 (2018), pp. 9451–9456.

[103] D. El Masri et al. "Dynamic light scattering measurements in the activated regime of dense colloidal hard spheres". In: *J. Stat. Mech. Theory Exp.* 2009.7 (2009).

[104] Paolo Sibani and Stefan Boettcher. "Mesoscopic real-space structures in spin-glass aging: The Edwards-Anderson model". In: *Phys. Rev. B* 98.5 (2018), pp. 1–13.

[105] Jesper Dall and Paolo Sibani. "Faster Monte Carlo simulations at low temperatures. The waiting time method". In: *Comput. Phys. Commun.* 141.2 (2001), pp. 260–267.

[106] Yuliang Jin and Hajime Yoshino. "Computer simulations of the Gardner transition in structural glasses". In: (2022), pp. 1–9. URL: http://arxiv.org/abs/2206.07868.

[107] Stefan Boettcher, Paula A. Gago, and Paolo Sibani. "Extreme fluctuations driving the relaxation in glassy energy landscapes". In: *Phys. A Stat. Mech.*

its Appl. 587 (2022), p. 126522. URL: https://doi.org/10.1016/j.physa.2021.126522.

[108] Camille Scalliet, Ludovic Berthier, and Francesco Zamponi. "Marginally stable phases in mean-field structural glasses". In: *Phys. Rev. E* 99.1 (2019), pp. 1–11.

[109] Camille Scalliet, Ludovic Berthier, and Francesco Zamponi. "Nature of excitations and defects in structural glasses". In: *Nat. Commun.* 10.1 (2019). URL: http://dx.doi.org/10.1038/s41467-019-13010-x.

[110] P.W Anderson, B.I Halperin, and C.M Varma. "Anamalous low-termperature thermal properties of glasses and spin glasses". In: *Philos. Mag. Struct. Prop. Condens. Matter* 25.1 (1972), pp. 1–9.

[111] W. A. Phillips. "Two-level states in glasses". In: *Reports Prog. Phys.* 50.12 (1987), pp. 1657–1708.

[112] P. R. Eastham et al. "Mechanism for the failure of the Edwards hypothesis in the Sherrington-Kirkpatrick spin glass". In: *Phys. Rev. B - Condens. Matter Mater. Phys.* 74.2 (2006), pp. 1–4.

[113] C. S. Nolle et al. "Effect of quenched disorder on moving interfaces in two dimensions". In: *Phys. A Stat. Mech. its Appl.* 205.1-3 (1994), pp. 342–354.

[114] P. J. Cote and L. V. Meisel. "Self-organized criticality and the Barkhausen effect". In: *Phys. Rev. Lett.* 67.10 (1991), pp. 1334–1337.

[115] V Meisel and P.J Cote. "Power laws, flicker noise, and the Barkhausen effect". In: *Phys. Rev. B* 46.17 (1992), pp. 822–828.

[116] Guang Ping Zheng, Mo Li, and Jinxiu Zhang. "Dynamics of Barkhausen jumps in disordered ferromagnets". In: *J. Appl. Phys.* 92.2 (2002), pp. 883–888.

[117] Matthieu Wyart. “Marginal stability constrains force and pair distributions at random close packing”. In: *Phys. Rev. Lett.* 109.12 (2012), pp. 1–5.

[118] Per Bak, Chao Tang, and Kurt Wiesenfeld. “Self-organized criticality”. In: *Phys. Rev. A* 38.1 (1988), pp. 364–374.

[119] Kevin P. O’Brien and M.B Weissman. “Statistical characterization of Barkhausen noise”. In: *Phys. Rev. E* 50.5 (1994), pp. 3446–3452.

[120] Djordje Spasojević, Stefan Graovac, and Sanja Janićević. “Interplay of disorder and type of driving in disordered ferromagnetic systems”. In: *Phys. Rev. E* 106.7 (2022), pp. 1–19.

[121] Johannes Falk, Marco Winkler, and Wolfgang Kinzel. “On the effect of the drive on self-organized criticality”. In: *J. Phys. A Math. Theor.* 48.40 (2015).

[122] Ferenc Pázmándi, Gergely Zaránd, and Gergely T. Zimányi. “Self-organized criticality in the hysteresis of the Sherrington-Kirkpatrick model”. In: *Phys. B Condens. Matter* 275.1-3 (2000), pp. 207–211.

[123] B. Gonçalves and S. Boettcher. “Hysteretic optimization for spin glasses”. In: *J. Stat. Mech. Theory Exp.* 2008.1 (2008).

[124] A. J. Bray and M. A. Moore. “Metastable states, internal field distributions and magnetic excitations in spin glasses”. In: *J. Phys. C Solid State Phys.* 14.19 (1981), pp. 2629–2664.

[125] Stefan Boettcher, Helmut G. Katzgraber, and David Sherrington. “Local field distributions in spin glasses”. In: *J. Phys. A Math. Theor.* 41.32 (2008).

[126] Josue X. de Carvarlho and Carmen P.C. Prado. “Self-Organized Criticality in the Olami-Feder Christensen Model”. In: *Phys. Rev. Lett.* 84.17 (2000), pp. 4006–4009.

[127] Scott Kirkpatrick. “Percolation and Conduction”. In: *Rev. Mod. Phys.* 45.4 (1973), pp. 574–588.

[128] S. Redner. “Percolation and conduction in a random resistor-diode network”. In: *J. Phys. A Gen. Phys.* 14.9 (1981), pp. 349–354.

[129] Ryan Jadrich and Kenneth S. Schweizer. “Percolation, phase separation, and gelation in fluids and mixtures of spheres and rods”. In: *J. Chem. Phys.* 135.23 (2011).

[130] Giacomo Rapisardi, Ivan Kryven, and Alex Arenas. “Percolation in networks with local homeostatic plasticity”. In: *Nat. Commun.* 13.1 (2022), pp. 1–9.

[131] P. Grassberger. “Numerical studies of critical percolation in three dimensions”. In: *J. Phys. A. Math. Gen.* 25.22 (1992), pp. 5867–5888.

[132] Carlo Baldassi et al. “Unreasonable effectiveness of learning neural networks: From accessible states and robust ensembles to basic algorithmic schemes”. In: *Proc. Natl. Acad. Sci. U. S. A.* 113.48 (2016), E7655–E7662.

[133] Marc Mezard. “Spin Glasses and Optimization”. In: *Europhys. News* 33.3 (2022), pp. 197–204.

[134] Hayato Goto, Kosuke Tatsumura, and Alexander R. Dixon. “Combinatorial optimization by simulating adiabatic bifurcations in nonlinear Hamiltonian systems”. In: *Sci. Adv.* 5.4 (2019), pp. 1–9.

[135] Hayato Goto et al. “High-performance combinatorial optimization based on classical mechanics”. In: *Sci. Adv.* 7.6 (2021), eabe7953.

[136] F. Romá et al. “The ground state energy of the Edwards-Anderson spin glass model with a parallel tempering Monte Carlo algorithm”. In: *Phys. A Stat. Mech. its Appl.* 388.14 (2009), pp. 2821–2838. URL: http://dx.doi.org/10.1016/j.physa.2009.03.036.

[137] William G. Macready, Athanassios G. Siapas, and Stuart A. Kauffman. "Criticality and parallelism in combinatorial optimization". In: *Science (80-.).* 271.5245 (1996), pp. 56–59.

[138] Kenneth Chang. "The Nature of Glass Remains Anything But Clear". In: *New York Times* (2008). URL: https://www.nytimes.com/2008/07/29/science/29glass.html.